

Received March 25, 2019, accepted April 3, 2019, date of publication April 11, 2019, date of current version April 22, 2019.

Digital Object Identifier 10.1109/ACCESS.2019.2909869

# Adaption Resizing Communication Buffer to Maximize Lifetime and Reduce Delay for WVSNs

WEI ZHANG<sup>1</sup>, WEI LIU<sup>2</sup>, TIAN WANG<sup>3</sup>, ANFENG LIU<sup>1</sup>, ZHIWEN ZENG<sup>1</sup>,  
HOUBING SONG<sup>4</sup>, (Senior Member, IEEE), AND SHAOBO ZHANG<sup>5</sup>

<sup>1</sup>School of Computer Science and Engineering, Central South University, Changsha 410083, China

<sup>2</sup>School of Informatics, Hunan University of Chinese Medicine, Changsha 410208, China

<sup>3</sup>College of Computer Science and Technology, Huaqiao University, Xiamen 361021, China

<sup>4</sup>Department of Electrical, Computer, Software, and Systems Engineering, Embry-Riddle Aeronautical University, Daytona Beach, FL 32114, USA

<sup>5</sup>School of Computer Science and Engineering, Hunan University of Science and Technology, Xiangtan 411201, China

Corresponding author: Zhiwen Zeng (zengzhiwen@mail.csu.edu.cn)

This work was supported by the National Natural Science Foundation of China under Grant 61572528, Grant 61772554, and Grant 6157256.

**ABSTRACT** Due to battery-powered wireless video sensor networks (WVSNs) takes on a high video data volume, it becomes a crucial issue to reduce energy consumption to maximize lifetime. At the same time, WVSNs are often applied to important situations for real-time and semi-real-time monitoring, thus ensuring the rapid transmission of these perceived data to sink is another critical issue. In static random-access memory (SRAM) communication buffer-based WVSN node, the radio is turned off during the data buffer-filling period as well as idle period. Because each radio transition contains the additional energy consumed by invalid packet header information and communication connection establishment, and the radio ON/OFF transition incurs extra circuit energy consumption. Therefore, from the perspective of saving energy, we need to reduce the ON/OFF transition frequency, which requires a large-sized buffer. However, the large size of SRAM buffer results in more energy consumption because SRAM energy consumption is proportional to the memory size. More importantly, the large ON/OFF transition frequency will lead to a large data transmission delay, which is harmful to applications. In this paper, an adaption resizing communication buffer (ARCB) scheme is proposed to maximize lifetime and reduce delay for WVSNs. In the ARCB scheme, the buffer size takes the minimum energy consumption optimization value in hotspot areas to maximize lifetime and takes a value smaller than the optimized value in non-hotspot areas to reduce delay. Although this consumes more energy for communication, since nodes in the non-hotspot areas have energy surpluses, it will not affect the lifetime. As a result, ARCB scheme can simultaneously increase the lifetime and reduce the delay in WVSNs. The effectiveness of the ARCB scheme is verified by theoretical analysis. The results show that the proposed ARCB scheme reduces the delay by 27.9%, and increases the effective utilization of energy by 24.1% under the condition that its lifetime is no less than previous schemes.

**INDEX TERMS** Wireless video sensor networks, buffer size, energy consumption, delay, lifetime.

## I. INTRODUCTION

With the rapid development of microprocessor technology [1], [2], its computing, communication and storage capabilities have multiplied, which makes sensor devices based on inexpensive microprocessors develop rapidly [3]–[4], and can potentially be applied to various fields, such as industrial monitoring [5], [6], crop monitoring [7], business information collection and recommendation

The associate editor coordinating the review of this manuscript and approving it for publication was Rui Xiong.

systems [8], ecosystems, environmental monitoring [9]–[11], traffic information [12]–[14], medical health [15]–[17], public safety [18]–[22], etc. [23]–[25]. Among them, Wireless Video Sensor Networks (WVSNs) is one of the fastest growing sensing devices [3, 26]. On the one hand, the increasing demand for public security makes wireless video sensor nodes more and more deployed in various buildings, roads and public places for 24-hour uninterrupted monitoring [27], [28], and the number of nodes deployed is extremely large [3], [26]. On the other hand, with the development of microprocessor technology, the volume of wireless video

sensor nodes is becoming smaller and smaller, while its sensing accuracy, computing and storage capacity have been doubled, thus greatly expanding its application areas, making it can be widely used in scenarios that used to be difficult to be deployed or applied [29]–[31]. Because nodes have the characteristics of wireless communication, which can be flexibly deployed, so it is widely deployed in the industrial production, agricultural crops, wildlife monitoring [26, [32]–[34]. These wireless video sensor nodes construct an important group of the Internet of Things (IoTs) [35], [36], with the decentralization trend of Internet [37], the emerging of Edge network [38], [39], Big data network [39] and Fog network [39], and combined with artificial intelligence [40], [41], wireless video sensor networks will usher in greater development.

The WWSNs sensor nodes usually consist of the following parts: a sensing component to sense various physical phenomena or events, CMOS image sensor (CIS) to obtain video data, video compressor to compress video data, communication component to transmit data, microcontroller, and a battery [3]. There are many challenges in WWSNs, and two issues are critical for the application of WWSNs [3], [26]. One of the challenging issues in WWSNs design is to reduce energy consumption and prolong lifetime because the video sensor nodes are battery-powered with limited energy. Another challenging issue is the delay, which is the time from the period when the packet is perceived to the period it is transmitted to the sink. It is obvious that the perceived video data should be transmitted to the sink as fast as possible, i.e. a small delay is required, so that the control center can respond quickly to the monitoring objects to effectively guarantee the development of applications [3], [26]. For example, in security monitoring, with the development of artificial intelligence technology, video data obtained by WWSNs combines with face recognition technology to automatically detect. When suspicious people or objects are found, security inspectors will be notified to go to the scene to deal with them in order to eliminate the danger. Therefore, it is of great significance to transfer video data quickly to control center, and delayed data transmission may result in safety accidents. In many applications, such as industrial production line monitoring, medical health monitoring applications [42]–[44], there are certain requirements for delay, requiring a very small delay, otherwise it may cause significant damage to the production workshop or people [45]–[47].

According to [3], the energy consumption components of WWSNs sensor nodes and their proportions are as follows: communication 70%, CMOS image sensor 8%, event Detector 1%, system controller 5%, and video encoder 16%. As can be seen from the above, the energy consumption for the communication accounts for about 70% of the total consumption [3, 48, 49]. Its energy consumption mainly includes energy consumption for data transmission, energy consumption for radio ON/OFF state transition, energy consumption for maintaining the function of SRAM buffer. Therefore, the focus of reducing energy consumption is to

reduce the energy consumption for communication. The main methods of reducing communication energy consumption are (a) Reducing the amount of data transmitted. This method is the most effective and direct method. Methods to reduce the amount of data, such as data compression [47], data fusion [47], data encoding [13], [14]. (b) Adjusting the duty cycle. In such methods, the energy consumption of video sensor nodes in awake state is thousands of times that of sleep state, so the method of duty cycle is to save energy by keeping them in sleep state when no communication is needed. The usual method is to let the radio remain OFF state during the data buffer-filling period or idle period, which can reduce energy consumption. But this method will increase the network delay. There are many studies to reduce the delay, such as: increasing the sending radius, cooperative routing and other strategies are for fast data collection.

However, the energy consumption of WWSNs nodes for communication has its particularity. Video sensor nodes first perceive the data, then store the perceived data into SRAM buffer. When the video content of SRAM buffer reaches a certain level, they open radio to transmit the stored video data to the sink [3]. Thus, the consumption for the communication includes the consumption of perception, the consumption of sending and receiving video data, the consumption of SRAM buffer, the radio ON/OFF transition incurs extra circuit consumption. Because the energy consumption of perceptual data is related to its application, it is not within the scope of this study. This paper mainly focuses on three kinds of communication consumption: (1) consumption of sending and receiving video data, (2) consumption of SRAM buffer, (3) the radio ON/OFF transition incurs extra circuit consumption [3]. The consumption of SRAM buffer is related to the size of buffer, because each memory cell needs electricity to maintain its storage activity, so the larger the size of buffer, the greater the energy consumption. In order to save energy, WWSNs nodes turn off radios when filling buffers to save energy. Many studies show that radios in idle state also consume a lot of energies [3]. Therefore, the communication consumption can be reduced as much as possible by turning on radio for data transmission after the video data is full of buffers. Obviously, in this case, the larger the buffer, the smaller the frequency of radio ON/OFF, which is beneficial to improving energy efficiency, because the conversion of radio from OFF state to ON state also requires additional circuit energy. Moreover, the larger the buffer, the more data is transmitted each time, and the less energy is consumed by communication links establishment and ineffective packet headers, so the communication energy consumption per bit is smaller. However, the larger the buffer, the greater the energy consumption of buffer maintenance, so the total energy consumption of video nodes is not necessarily the smallest at this time. Choi *et al.* [3] conducted a study on the optimization of the size of buffer. The study found that: when the buffer is small, the energy consumption in the buffer itself is small, but the frequency of radio ON/OFF is high, so the energy consumption consumed in the data transmission

is high. As the buffer increases, the consumption of the buffer itself increases, but since the frequency of the radio ON/OFF decreases, the energy consumption spent on data transmission is greatly reduced. Thus Choi *et al.* [3] gives the value of the buffer size when the consumption of video nodes is minimal.

However, Choi *et al.* [3] only studied the optimal value of energy consumption, did not realize that the size of buffer will affect the network delay. From the perspective of reducing the delay, it is desirable that the value of the buffer is as small as possible. When the buffer is large, it takes longer for the video data to fill the buffer, which increases the delay, especially when multi-hop routing, each hop will increase delay, so end to end delay grows more significantly.

It can be seen that when the size of buffer gets the optimal value, its delay may get a larger value. Therefore, how to tradeoff between energy consumption and delay is worth studying. However, delay increases monotonously with the increase of buffer, and the relationship between energy consumption and buffer size is: when the buffer is small, frequent radio operations will lead to large energy consumption; when buffer size is large, the energy consumption of maintaining buffer itself is also large. Therefore, we can take an intermediate optimization value for the buffer size, then the delay and energy consumption of WVSNS can be optimized simultaneously. In this paper, we carefully studied the energy consumption characteristics of WVSNS and proposed an Adaption Resizing Communication Buffer (ARCB) scheme to maximize lifetime and reduce delay simultaneously for WVSNS. The main innovations of this paper are as follows:

(1) First, the relationship between the delay and the size of buffer, the energy consumption relationship between the delay and video nodes are deduced theoretically in WVSNS. Thus, the trade-off optimization relationship between delay and energy consumption is theoretically given. In addition, the energy consumption characteristics of WVSNS are also analyzed and obtained, which lays a theoretical foundation for the proposed ARCB scheme.

(2) An Adaption Resizing Communication Buffer (ARCB) scheme is proposed to maximize lifetime and reduce delay simultaneously for WVSNS. Based on the relationship of the delay, the size of buffer and the energy consumption, in ARCB scheme, the buffer size in the hotspots region is taken an optimal value that can make the energy consumption minimal because the energy consumption in hotspots determines the lifetime of the whole network. And the buffer size of non-hotspots takes a value smaller than the optimized value in hotspots. Its purpose is to make the buffer size as small as possible under the premise that the energy consumption of nodes is not greater than that of the hotspots region, so that the delay of the non-hotspot region is minimized. Therefore, under ARCB scheme, the delay decreases significantly and the network lifetime is the same as the previous studies. To the best of our knowledge, previous studies only considered the minimum energy consumption of the network and did not optimize the delay at the same time. This paper not only considered the energy consumption and delay, but also

realized the optimization of maximizing network lifetime and reducing delay simultaneously for the first time, which was not achieved in previous studies.

(3) We provide extensive theoretical analysis to confirm the effectiveness of the proposed ARCB scheme. In experimental comparison, for medium scale sensor networks, ARCB scheme can reduce delay by 27.9% at the same time maximizing network lifetime, and improve the effective utilization of energy by 24.1%.

The rest of this paper is organized as follows: Section II reviews related works comparing with ARCB scheme. Section III describes the network model and defines problem statements of this paper. In Section IV, the design of ARCB scheme is presented for WVSNS. The results of the theoretical analysis are given in Section V. We conclude this paper in Section VI.

## II. RELATED RESEARCH

Energy consumption and lifetime have always been the research focus in WVSNS. Researchers have proposed many different energy-saving strategies and methods for the variety of energy consumption of sensor nodes [2], [25], [27], [35], [46], [47]. In fact, energy consumption and lifetime are closely related but not identical indicators. It cannot be simply said that reducing energy consumption will certainly improve lifetime [3], [28], [44]. Lifetime is the death time of the first node in the network, so the most effective way to improve the lifetime is to reduce the largest energy consumption in the network [3], [28], [44].

### A. BUFFER SIZE, ENERGY CONSUMPTION AND DELAY RELATED BUFFER

Reference [3] studies the relationship between the size of buffer and energy consumption, and the relationship between the size of buffer and energy consumption of data transmission. The conclusion of their work is that the larger the buffer, the smaller the energy consumption of data transmission. But the greater the energy consumed by the buffer itself. Choi *et al.* [3] studies the energy consumption of data transmission and the energy consumption of buffer itself, and then obtain the value of the buffer size which minimizes the total energy consumption. Their results show that when size of buffer is small, the energy consumption of the node for data transmission is large, which leads to the total energy consumption of the node is large. When buffer size is large, although the energy consumption of data transmission is effectively reduced, the total energy consumption of nodes is large because of large energy consumed by the buffer itself. Therefore, the optimal buffer size generally takes a moderate value.

Although Choi *et al.* [3] gives the optimal buffer size, their work only considers the buffer size in terms of energy consumption. Although energy consumption is an important performance of WVSNS, the delay is also an important indicator for WVSNS. Therefore, a good scheme should optimize the energy consumption of WVSNS and delay simultaneously.

The relationship between delay and buffer size is approximately linear. The smaller the buffer, the smaller the delay.

## B. ENERGY CONSUMPTION AND LIFETIME RELATED WORK

In WWSNs, nodes are generally powered by batteries [2], [25], [27], [35], [46], [47]. Due to cost and volume constraints, the battery capacity of nodes is generally small [2], [25], [27], [35]. Therefore, how to reduce the energy consumption of nodes and extend lifetime of network has become an important content of wireless sensor networks (WSNs) [3], [28], [44]. For Wireless Video Sensor Networks (WWSN), the energy consumption of sensor nodes is composed of different components. In order to reduce the energy consumption of nodes, corresponding work should be done for different energy-consuming components to reduce their energy consumption. According to [3], the energy consumption of data transmission accounts for the largest part of the energy consumption of WWSN sensor nodes. The most effective way to reduce the energy consumption of sensor nodes is to reduce the energy consumption of data transmission.

Among them, data fusion is the most popular and effective method. The main idea is that the perceived data between sensor nodes are correlated spatially and temporally [47]. For example, videos transmitted by video nodes are highly correlated in the time dimension. When the time is close, the background of adjacent videos is almost the same, there is correlation between video data. Spatially, there is also a correlation between the perceived video data between sensor nodes not far away from each other. Therefore, data aggregation can be performed when data with correlation is aggregated at the same node in the process of routing to sink. Consequently, energy consumption can be effectively saved. There are many methods to reduce data fusion based on data aggregation. These data aggregation schemes can be divided into routing-driven schemes, fusion-driven schemes and coding-driven schemes. The main goal of routing-driven schemes is to design effective routing. The representative strategy of the routing-driven schemes is LEACH routing strategy [50]. It distributes network nodes into clusters, each cluster has a node called cluster head, and the rest of the nodes are cluster members. Member nodes send their own data to cluster head. Cluster head fuses the data within the cluster and sends it to sink, so that the data needed to be sent can be greatly reduced. Fusion-driven schemes are the most widely used data aggregation scheme. The main purpose of this method is to maximize data fusion and reduce the amount of data that the network needs to transmit. In general, shortest routing is the most commonly used routing strategy. However, in data aggregation routing, if the data packet arrives at sink along the shortest path, it will be difficult for the data packet to meet in the routing process, thus the probability of fusion is low, and the data amount forwarded by the node will be larger. Therefore, in data fusion routing strategies such as fusion-driver, routing to sink is designed based on maximum probability of data encounter. Under this guidance,

the routing of data packets will not be completely oriented to sink, but along the route that may maximize the probability of data packet encounter, to minimize the amount of data that node undertakes. Coding-driven schemes [52]–[54] is another strategy for reducing data volume. This kind of strategy mainly reduces the data amount that needs to send through data encoding. Including distributed source coding schemes (e.g. Slepian-Wolf coding model) [52]–[54] and explicit side-information aggregation [54].

Data convergences is a special data aggregation strategy. In this strategy,  $n$  packets will be merged into one packet when they meet. In the data aggregation network discussed above, the nodes in the near sink region bear more data than those in the far sink region, so the energy consumption of the whole network is unbalanced. In data convergences data collection network, each node receives all data packets and fuses them into one data packet, then sends them one time, so the energy consumption of nodes is basically equal. Therefore, the focus of this kind of strategy is how to collect the data of the whole network with the smallest delay. There are many studies in this area. The commonly used method is a distributed algorithm, which is somewhat like cluster network. In previous studies, the size of each cluster was equal. Li *et al.* [31] believed that the data aggregation delay of the network structure of the same cluster was large. Later, a novel unequal cluster data convergences structure is proposed. In its proposed network structure, the so-called "far-small-near-large" unequal cluster network structure has proposed, and the larger cluster radius is used in near sink region and smaller cluster radius is used in far sink region. The strategy proposed by Li *et al.* [27] is like that proposed in this paper. ON/OFF conversion of the radio of video nodes requires the same energy consumption. In data aggregation, the transition of nodes from sleep to work state also requires energy consumption. Therefore, the state transition from sleep to work should save energy. In data aggregation, each node receives data packets multiple times, but only one operation of data transmission is needed. Therefore, the ideal situation is that in a round of data collection, the node changes from sleep to work state, completes all data operations as little time as possible, and then change to sleep state. The network structure of unequal cluster radius proposed by Li *et al.* [27] makes it possible for nodes to carry out state transitions only once in each round of data collection. In their strategy, the sensor nodes with consecutive time slots are scheduled ingeniously for reducing the number of state transitions by postponing the data collection time of clusters with smaller degree, so that the node only needs one state in a round of data collection, which effectively improves the network lifetime.

## C. DUTY CYCLE-BASED DELAY RELATED WORK

Duty cycle mechanism is a strategy commonly used to save energy [33], [44]. In such a strategy, sensor nodes periodically wake up and sleep. Because the energy consumption of waking up is several orders of magnitude lower than that of the sleep state, it is necessary to make the node in the sleep state

as much as possible to save energy. However, nodes cannot send and receive data when they are sleeping, which has an impact on network performance, especially on delay. Because when sender has data packets to send, if the receiver is sleep, sender needs to wait for the receiver to be awake up, thus increasing delay. Fortunately, in wireless sensor networks, there are many sensor nodes deployed, therefore, when sender sends data, there may be several nodes closer to sink that act as forwarding nodes, one of these forwarding nodes can forward data when it is awake, so the delay is smaller than the worst case. In this case, sender chooses the node nearest to sink as receiver, which can transmit data to sink with the minimum number of hops. From the above discussion, it can be seen that the duty cycle of the node will increase the delay of data transmission. Liu *et al.* [55] studied the relationship between delay and duty cycle. They found that when a node has data to transmit, if the node nearest to sink in the forward node set is in the awake state, it is the best case to select the node to transmit data. However, in most cases, when sender sends data, the nearest node to sink is sleep. Therefore, sender has two choices: one is to select a node nearest to sink in the awake state as relay node for data transmission; the other is to wait for the node nearest to sink to wake up and then use it as relay node for data transmission. In the first method, although there is no need to wait, the nodes that may be selected make the distance from one hop to sink smaller, and the whole routing needs more hops so that the total delay is not small. In the second method, because the node awake/sleep is random, it may lead to a longer waiting time, which makes the data transmission delay larger. Liu *et al.* [55] proposed a scheme named FFSC scheme that can reduce delays and maintain high lifetime. In FFSC scheme, for nodes in far sink region, because of its enough energy, node chooses nodes in waking up state to forward data. Although this may consume more energy, it does not affect network lifetime because of the energy surplus of nodes in far sink region. For the area near sink, it chooses the node nearest to the sink as the relay node. Therefore, FFSC has better performance on delay and lifetime.

For WVSNSs, there are two ways to choose radios, one is called Persistent Idle Mode (PIM) and the other is called Energy Saving Mode (ESM). Choi *et al.* [3] pointed out that the 802.11g (Wi-Fi) radio power consumption for transmission (Tx), receiving (Rx), and IDLE state was 303.6 mW/617.1 mW/230 mW, respectively. When radios are idle, their energy consumption is close to the energy consumption of receiving data and half of the energy consumption of sending data. Therefore, in WVSNSs, when video nodes adopt PIM mode, the nodes are always in awake state. When there is less data in buffer, radio is in idle state. When data filling in buffer reaches a certain degree, the radio converts to sending/receiving (ON) state and forwards data. The advantage of PIM mode is that the system always detects the buffer, once the buffer capacity meets the minimum transmission condition, the data in the buffer will be sent out, so that the data will stay in the buffer for a short time, so that

the perceived data can be sent to sink with a smaller delay. But PIM mode consumes a lot of energy because radios are always idle. Especially in those networks with small data generation, it takes a long time to fill buffer into a certain data at a time, so radios mostly keep idle state, thus consuming a lot of energy. In ESM mode, radio is not always in awake state, but in sleep state before the buffer is full to save energy. When the buffer is full of data, radio is turned on for data transmission. The advantage of ESM mode is that if the size of buffer is large, filling buffer takes a longer time, radios can stay in sleeping state for a longer time, thus saving energy. But the disadvantage is that the data transmission of radio is interval. When the buffer is large, the delay of data transmission will be larger, and the larger the buffer, the more energy consumed by the buffer itself. In addition, radios require intermittent state transitions from sleep to awake, which also require energy consumption. According to [3], the start-up time of radio from sleep to work is 1.3s, and the energy consumed for start-up is 299mJ. Therefore, Choi *et al.* [3] gave the calculation method of optimized buffer size.

As a protocol of MAC layer, duty cycle mechanism plays an important role in energy consumption [3], [33], [44]. The awake time of a node in a cycle is also related to the amount of data the node undertakes. The more data the node undertakes, the longer awake time in a duty cycle. Based on the above analysis, in order to reduce the energy consumption of nodes, some researchers proposed an adaptive duty cycle method to reduce the energy consumption of nodes [25]. They adopt the method that the awake time of a node in a cycle is determined by the amount of data that the node undertakes. If the amount of data that the node undertakes is large, the waking up time will be long. On the contrary, when the amount of data that the node undertakes is small, the awake time of the node in a cycle will be short, so as to save energy. Although this strategy can save energy as much as possible, its delay is not optimal. In [7], the waking time of nodes in near-sink region is longer than that in far-sink region. Although this reduces the energy consumption of the whole network, it does not improve the network lifetime, because lifetime is determined by the maximum energy consumption in the network. On the contrary, delays increase because of the decrease of awake time of nodes in the far sink region. Based on the above analysis, Chen *et al.* [56] proposed a new strategy. The main point of their strategy is to increase the awake time of nodes by using the remaining energy. In this way, although the energy consumption of these nodes is increased, the network lifetime of these nodes is not affected.

#### D. RESEARCH ON OTHER DELAY OPTIMIZATION

In fact, there are many approaches to reduce delay in WSNs/WVSNSs. It can be optimized by MAC, network layer and data transmission layer, and it can also be optimized from multiple levels at the same time.

Firstly, it is discussed from the MAC layer. Related to this study is the duty cycle mechanism [3], [33], [44], [56]. Although the longer awake time in a cycle, the smaller

the delay. But this kind of method is at the cost of energy consumption, which limits its use. Therefore, the ideal scenario is to reduce delay without increasing the awake time of nodes. In fact, it is possible in duty cycle based WWSNs, the nodes are divided into synchronous network and asynchronous network. At the same time, the duty cycle between nodes is synchronized, that is, the nodes in the same slot wake up at the same time for data transmission, while other slots sleep at the same time, and the time between nodes is not offset. It can be seen that the slot of synchronous network can be predicted, so a smaller delay routing strategy can be designed. However, the synchronous network needs interaction between nodes to adjust the time to prevent time offset between nodes, which requires a large system cost, and for large networks, the cost of maintaining time synchronization is higher. The other is asynchronous network, in which each node has its own wake up time, so the slots of nodes wake up or sleep may be different. The advantage of this asynchronous network is that the nodes do not need to maintain synchronization, so the network system has low cost and good scalability. However, because each node decides whether to awake independently, the active slot of the node is random. When sender needs to transmit data, its receiver is in sleep state, which makes sender need to wait for it waking up to transmit data, so the delay is increased. Wu *et al.* [57] proposed a local synchronization method which can effectively reduce the delay while the cost of the system is relatively low. The idea of their strategy is that, because of the large number of sender nodes deployed, when sender sends data, there are several nodes close to sink and within the transmission range of sender that can act as receivers. Therefore, when sender and receiver are synchronized, the receiver corresponding to sender awake is also in the awake state, which reduces the possible waiting time and delay. The advantage of their method is that it does not require all nodes in the whole network to synchronize, but only loosely synchronize the associated nodes. Therefore, the cost of the system is very low, easy to implement, and the reduction of delay is very effective.

There are also many studies to reduce delay by designing transport protocols. In WWSNs, because of wireless transmission, the bit error rate of wireless transmission is much higher than that of wired network. Therefore, many data transmission protocols used in wired networks are unsuccessful in wireless networks, for example, the send and wait automatic repeat-request (SW-ARQ) protocol [58]. In SW-ARQ protocol, sender waits after sending the data packet, and receiver responds to Acknowledge (ACK) signal after receiving the data packet to indicate that the data packet has been received. When sender receives the ACK signal, it knows that the packet has been successfully sent to receiver, and then sender starts sending the next packet. If the packet is lost during transmission, sender will not receive ACK signal, and sender will send the packet again. The above process is repeated until the packet is successfully sent, or when the maximum number of repeats reaches the upper limit, the transmission of the packet is abandoned. It can be seen that SW-ARQ

protocol needs multiple retransmissions when the communication link is not good, which makes the transmission delay larger. In addition, SW-ARQ protocol is sent serially to each data packet, so its throughput and delay are relatively large. The following improvement strategies are proposed: Go back-N (GBN) protocol and Selective repeat (SR) protocol [58]. The main feature of these improved protocols is that sender can send  $K$  packets in one time, and receiver can report the last received packet ID to sender, or not received data ID to make sender know which packets have been successful or which packets need to be retransmitted. Obviously, GBN and SR protocol can effectively improve data transmission performance.

In fact, the main reason for the above data transmission delays is that the packet loss rate exists in the wireless communication link, which results in data retransmitting, leading to a large delay. Another way to reduce delay is to improve the success rate of data transmission. An effective way to improve the success rate of data transmission is to increase the transmission power of the node and increase the signal-to-noise ratio (SNR) of the receiver. But this will increase the energy consumption of nodes and reduce lifetime. Chen *et al.* [59] analyzed the energy required for transmitting unit bit data packets at different transmission powers and set the transmission power that minimized the unit bit energy consumption for data transmission.

Data encoding mechanism is also an effective way to reduce delays. The idea is that sender redundantly encodes data packets [52], [53] before sending them, so that receivers can successfully recover data even if they miss part of the data. Data encoding mechanism improves the reliability of data transmission, reduces the number of data packets retransmitted, and can effectively reduce delay. But the shortcoming is that it adds some redundant checking data to the package when encoding, so the encoding data package is larger than the original data packet. Therefore, although this method reduces the delay, it will increase the amount of data that the node needs to transmit and reduce the lifetime. Zhang and Liu [60] proposed a better strategy to reduce delays without reducing lifetime. Their strategy is to adopt high redundancy coding in far-sink areas, because there is a lot of energy surplus in these areas, so it will speed up data transmission but not affect lifetime.

From the above discussion, we can see that the energy consumption and delay of WWSNs include many levels. The largest energy consumption of video nodes is in communication. Energy consumption of communication includes the energy consumption of transmitting data, receiving data, idle waiting, the energy consumption of radio state transition, and the energy consumption of buffer itself. Delay includes one-hop delay and end-to-end delay. Therefore, it has great challenge to optimize energy consumption and delay simultaneously. The proposed Adaption Resizing Communication Buffer (ARCB) scheme attempts to make a beneficial attempt for simultaneously maximizing lifetime and reducing delay in WWSNs.

III. SYSTEM MODEL

A. NETWORK MODEL

Wireless Video Sensor Networks (WVSNs) in this paper is similar to the network model adopted in [3]. In such networks,  $n$  wireless video nodes are deployed in a network with a network radius of  $R$ , nodes density of  $\rho$ , and the location of these nodes cannot be changed after deployment. One special node called sink is located in the network center, and the energy of the sink node is supplied by active power, its energy is infinite. While other video nodes are powered by batteries, and their energy is limited. The main function of video sensor nodes is to monitor the surrounding environment and capture video or other forms of data and send the perceived data to the sink node through multiple hops. Then the sink node connects with Internet through wired networks, so that the perceived data can be timely transmitted to Control Center. Finally, Control Center analyses the perceptual data and processes the abnormal events in time. The network model adopted in this paper can be illustrated by Figure 1.

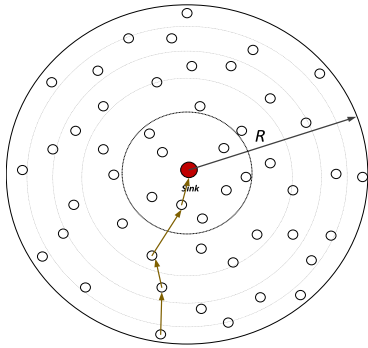


FIGURE 1. The network model of WVSNs.

B. NODE MODEL

Similarly, the node model used in this paper is similar to [3]. Video sensor nodes are composed of the following components: event detector, image sensor, system controller, video encoder and communication block. After the event detector detects the event, the system is awakened by the system controller. Then the image sensor captures and collects the video for coding and compression. The collected and received video data are temporarily stored in the communication buffer and waiting to be sent to other nodes, as shown in Figure 2. Communication block includes radio and communication buffer. In order to save energy, node adopts energy-saving model (ESM), that is, when image sensor perceives that buffer is being filled with data contents, nodes shut down radio to save energy. When the data of buffer is full, nodes wake up radio to send data. Therefore, radio is closed when there is no data communication in ESM. However, when the communication buffer is filled with data, there is no data transmission, so the delay of data transmission is larger. When the communication buffer is full, it needs to wake up the radio to communicate, which also consumes a small amount

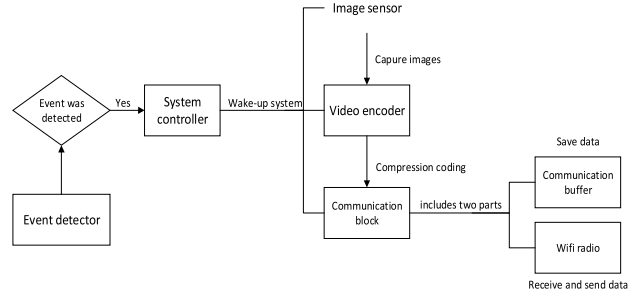


FIGURE 2. The control model of WVSNs nodes.

of energy and has a certain time delay. Therefore, the goal of this paper is to maximize lifetime while minimizing delay.

C. ENERGY CONSUMPTION MODEL

Because the communication block is the most energy-consuming module and the most important module affecting data transmission, so like Ref. [3], we focus on the influence of communication block on energy consumption and delay. According to Ref. [3], when the energy consumption of event detector, image sensor, system controller and video encoder is determined, the energy consumption of communication block mainly includes the energy consumption of communication buffers and the energy consumption of radio startup and data transmission, as shown in Eq.1.

$$\omega_{sum} = 2 \cdot \omega_s + \omega_c \tag{1}$$

Among them,  $\omega_{sum}$  is the total energy consumption of communication block;  $\omega_s$  is the energy consumption of communication buffer;  $\omega_c$  is the energy consumption for start-up, data receiving and data sending of radio. It should be noted that when transmitting data, the total consumption includes receiving data and sending data, so the sum of energy consumption of radio should be calculated twice.

According to Ref. [3], the energy consumption of communication buffer includes: (1) the leakage energy consumption of communication buffer  $\omega_{sl}$ , which is the product of the leakage power  $p_{sl}$  and the duration time (2) the energy consumption of reading or writing data in communication buffer  $\omega_{sd}$ , which is the product of the reading and writing consumption for each byte data  $e_{sd}$ , the video data size in per second  $C_{vs}$ , and the event duration time  $t_a$ . Thus, the energy consumption of communication buffer can be expressed by Eq. 2. The specific meaning of symbols in the formula is shown in Table 1.

$$\omega_s = \omega_{sl} + \omega_{sd} = p_{sl} \cdot t_a + e_{sd} \cdot C_{vs} \cdot t_a \tag{2}$$

Under the energy-saving model, then nodes are filling buffer, radio turns off to save energy. After the buffer is full, radio start up and adjust its state to ON (sending/receiving), when the data is transmitted, the radio turns off again. Suppose the event duration time is  $t_a$ , so the data volume generated is  $C_{vs} \cdot t_a$ . When the buffer is full, the bandwidth is  $C_{bw}$ , the speed of filling buffer is  $C_{vs}$ , so the time required for transmitting buffer-sized data is  $t_b$ , and  $t_b$  satisfies

TABLE 1. Symbols related to calculation.

Symbol	Description	Value
$\omega_{sum}$	Energy consumption of communication block	Calculation
$s_{sram}$	Communication buffer size	Calculation
$s_{opt}$	Optimum size of communication buffer	Calculation
$s_{xn}$	Communication buffer size of the node from sink x meters	Calculation
$s_x$	Appropriate communication buffer size of the node from sink x meters in new scheme	Calculation
$C_{vs}$	Size of coded video data per second	Calculation
$C_{bw}$	Bandwidth of wireless channel	16-54Mbps
$\omega_s$	Energy consumption of communication buffer	Calculation
$\omega_{sd}$	Dynamic energy consumption of communication buffer	Calculation
$\omega_{st}$	Leakage energy consumption of communication buffer	Calculation
$e_{sd}$	Energy consumption of reading or writing each byte data in communication buffer	Calculation
$p_{sl}$	Leakage power of communication buffer	Calculation
$t_a$	Duration of the event	30s/60s
$\omega_c$	Total energy consumption of radio	Calculation
$\omega_{cs}$	Energy consumption of radio for start-up	299mJ
$\omega_{ct}$	Energy consumption of radio for sending and receiving data	Calculation
$\omega_{ci}$	Energy consumption in the idle state	Calculation
$\omega_{cb}$	Energy consumption in transferring and receiving buffer-sized data	Calculation
$\omega_{cr}$	Energy consumption for transferring and receiving remaining data less than one buffer size	Calculation
$p_{ci}$	Idle power	230mW
$p_{ctr}$	Receiving power	303.6mW
$p_{ctt}$	Transmitting power	617.1mW
$p_{ct}$	Sum of receiving power and transmitting power	920.7mW
$t_{ca}$	Start-up time of radio	1.3s
$a_{rd}$	Residual energy of less than one buffer size	Calculation
$t_b$	Time required to transmit buffer-sized data	Calculation
$t_{com}$	Communication cycle	100ms
$t_x$	One-hop delay of the node from sink x meters	Calculation
$t_{xe}$	End-to-End delay of the node from sink x meters	Calculation
$\mathcal{D}_{sink}^x$	End to sink delay	Calculation
$\mathfrak{J}$	Network lifetime	Calculation

$t_b C_{bw} - t_b C_{vs} = s_{sram}$ , then  $t_b = s_{sram} / (C_{bw} - C_{vs})$ . The data transmitting and receiving power is  $p_{ct}$ , then the energy consumption for transmitting one-buffer-sized data

TABLE 2. List of abbreviations.

Abbreviation	Description
WVSNs	WVSNs wireless video sensor networks
ARCB	Adaption Resizing Communication Buffer
FBSA	Fixed Buffer Size Adjustment
OBSA	Optimum Buffer Size Adjustment
PIM	Persistent Idle Mode
ESM	energy saving model
CIS	CMOS image sensor
SRAM	static random access memory
ACK	Acknowledge
SR	Selective repeat
GBN	Go back-N
SNR	signal-to-noise
App_ESM	the mode that nodes adopt the optimal size under the ESM mode

is  $p_{ct} \cdot t_b$ . When the event occurs, the number of start-up times of the radio (e.g. the number of filling buffers) is  $n = \lceil (C_{vs} \cdot t_a) / (C_{bw} \cdot t_b) \rceil$ . Since the energy consumption of transmitting an event data is the sum of the energy required by the node to start radio and transmit data. The energy consumption for radio start-up is  $\omega_{cb}$ , the data transmitting and receiving power is  $p_{ct}$ , then the energy consumption for transmitting buffer-sized data is  $\omega_{cb} = 2 \cdot \omega_{cs} + p_{ct} \cdot t_b$ , and the energy consumption of transmitting residual data  $a_{rd}$  is  $\omega_{cr} = 2 \cdot \omega_{cs} + p_{ct} \cdot a_{rd} / C_{bw}$ , so the total energy consumption for transmitting an event data is shown in Eq. 3.

$$\begin{aligned} \omega_c &= n \cdot \omega_{cb} + \omega_{cr} \\ &= n \cdot (2 \cdot \omega_{cs} + p_{ct} \cdot t_b) + 2 \cdot \omega_{cs} + p_{ct} \cdot \frac{a_{rd}}{C_{bw}} \end{aligned} \quad (3)$$

#### D. PROBLEM STATEMENT

The goal of this paper is to find a reasonable buffer size to maximize the network lifetime and minimize the delay. Suppose the buffer size of the node whose distance from sink is x meters is  $s_x$ , then the goal of this paper is to find a suitable set of  $s_x | x \in \{1..500\}$ , which are the following two objectives.

(1) End to sink delay ( $\mathcal{D}_{sink}^x$ ). End to sink delay represents the time period between sending a packet from a node with distance x meters to sink and receiving a packet successfully by the sink.  $\mathcal{D}_{sink}^x = \sum_{i=0}^k \mathcal{D}_i^x$ , here k represents the number of hops in the whole transmission process,  $\mathcal{D}_i^x$  is a function of  $s_x$  and represents the time of the  $i^{th}$  hop. Because the smaller the End to sink delay, the better, so it can be represented as Eq. 4

$$\min(\mathcal{D}_{sink}^x) = \min\left(\sum_{i=1}^k \mathcal{D}_i^x\right) \quad (4)$$

Network lifetime ( $\mathfrak{J}$ ). Generally speaking, network lifetime is the lifetime of the first dead node in the network, so the most effective way to improve the lifetime of the network is to



minimize the energy consumption of the node with the largest energy consumption [3], [28], [44]. Suppose the initial energy of nodes in the network is  $E_{tot}$ , and the energy consumption per unit time of the node from sink  $x$  meters is  $\varepsilon_x$ , so lifetime can be represented by Eq.5 and Eq.6.

$$\mathcal{J} = \frac{E_{tot}}{\max(\varepsilon_x)} \quad (5)$$

$$\max(\mathcal{J}) = \frac{E_{tot}}{\min(\max(\varepsilon_x))} \quad (6)$$

In summary, our optimization objectives can be expressed as Eq.7

$$\begin{cases} \min(\mathcal{D}_{sink}^x) = \min(\sum_{i=1}^k \mathcal{D}_i^x) \\ \mathcal{J} = \frac{E_{tot}}{\max(\varepsilon_x)} \\ \max(\mathcal{J}) = \frac{E_{tot}}{\min(\max(\varepsilon_x))} \\ \mathcal{D}_{sink}^x \leq \mathcal{D}^\theta, \mathcal{J} \geq \mathcal{J}^\theta \end{cases} \quad (7)$$

Here,  $\mathcal{D}^\theta, \mathcal{J}^\theta$  represent the minimum requirement for performance values in network. The function of Eq.7 is to maximize network lifetime and minimize transmission delay while meeting the minimum requirements of network performance value.

#### IV. DESIGN OF ARCB SCHEME

##### A. RESEARCH MOTIVATION

Communication block consumes the most energy of nodes, which mainly includes the energy consumption of communication buffer and the energy consumption of radio. In order to reduce energy consumption and improve network lifetime, according to the previous network model, when filling buffer, its data sources are not only the perceived data of the node itself, but also data sent to sink by other nodes and relayed by the node, at this time the radio is in the OFF state. When the buffer is full, the radio is restarted for transmission. Because switching the radio also consumes energy, in order to reduce energy consumption, the radio startup times should be reduced as much as possible to reduce energy consumption. Therefore, the larger the buffer, the fewer the radio startup times, and the less energy the radio consumes. However, the buffer itself also consumes energy, and its energy consumption is proportional to the size of the buffer.

Choi et al. [3] calculated the power consumption of buffers with different capacities by CACTI tool. The data showed that the dynamic power and leakage power increased approximately proportionally with the increase of buffer size. The dynamic power consumption and leakage power consumption could be expressed by Eq. 8 and Eq. 9. The calculation model is fitted by MATLAB, and  $A_1, A_2, B_1, B_2$  are fitted constants.

$$e_{sd} = A_1 \cdot s_{sram} + A_2 \quad (8)$$

$$p_{sl} = B_1 \cdot s_{sram} + B_2 \quad (9)$$

The parameters in the equation are consistent with the energy consumption data of communication buffer obtained

from CACT, so  $A_1 = 2.15 \cdot 10^{-17}, A_2 = 2.06 \cdot 10^{-12}, B_1 = 1.93 \cdot 10^{-8}, B_2 = 0.00011$ . Combining with Eq. 2, Eq. 8 and Eq. 9, the Eq. 10 is obtained, which is the energy consumption of the communication buffer  $\omega_s$  based on the size of the communication buffer ( $s_{sram}$ ).

$$\omega_s = s_{sram} (A_1 \cdot C_{vs} \cdot t_a + B_1 \cdot t_a) + A_2 \cdot C_{vs} \cdot t_a + B_2 \cdot t_a \quad (10)$$

Setting image parameters are (CIF, 30fps, 0.6bpp), the energy consumption of communication buffer is shown in Figure 3. Because the order of magnitude of  $A_1, A_2$  is small, here, the influence of channel bandwidth is neglected.

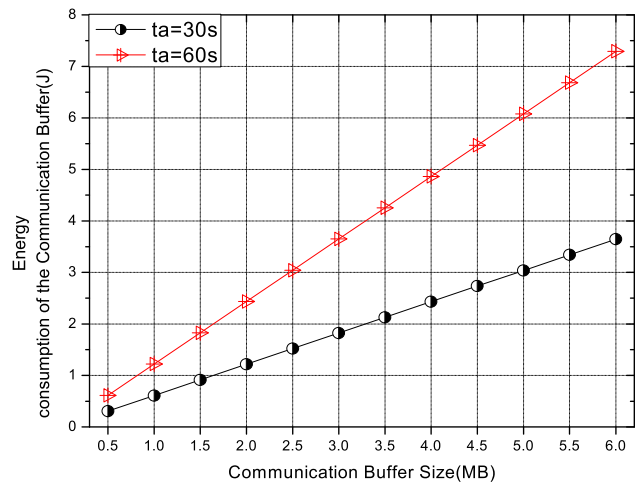


FIGURE 3. Energy consumption of communication buffer with different buffer size.

As mentioned in the previous energy consumption model, the energy consumption of radio in communication is mainly the energy required for data transmission and radio start-up. Suppose the event duration time is  $t_a$ , so the data volume generated is  $C_{vs} \cdot t_a$ . When the buffer is full, the bandwidth is  $C_{bw}$ , the speed of filling buffer is  $C_{vs}$ , so the time required for transmitting buffer-sized data is  $t_b$ , and  $t_b$  satisfies  $t_b C_{bw} - t_b C_{vs} = s_{sram}$ , then  $t_b = s_{sram} / (C_{bw} - C_{vs})$ . The data transmitting and receiving power is  $p_{ct}$ , then the energy consumption for transmitting one-buffer-sized data is  $p_{ct} \cdot t_b$ . When the event occurs, the number of start-up times of the radio (e.g. the number of filling buffers) is  $n = \lceil (C_{vs} \cdot t_a) / (C_{bw} \cdot t_b) \rceil$ , and the energy consumption for each start-up is  $\omega_{cs}$ , the amount of data left that is not enough to fill a buffer is  $a_{rd} = C_{vs} \cdot t_a - n \cdot C_{vs} \cdot t_b$ , the energy consumption for the left data is  $a_{rd} \cdot \frac{a_{rd}}{C_{bw}}$ . Then, combining with Eq. 3, the energy consumption of radio based on buffer size can be obtained, as shown in Eq.11.

$$\omega_c = 2 \cdot \omega_{cs} \cdot C_{vs} \cdot t_a \cdot \frac{C_{bw} - C_{vs}}{C_{bw} \cdot s_{sram}} + p_{ct} \cdot \frac{C_{vs} \cdot t_a}{C_{bw}} + 2 \cdot \omega_{cs} + \frac{C_{vs} \cdot p_{ct}}{C_{bw}} \cdot \left( t_a - \frac{C_{vs} \cdot t_a}{C_{bw}} \right) \quad (11)$$

According to the Eq. 11, the energy consumption of the radio with different buffer size can be calculated, as shown in Figure 4.

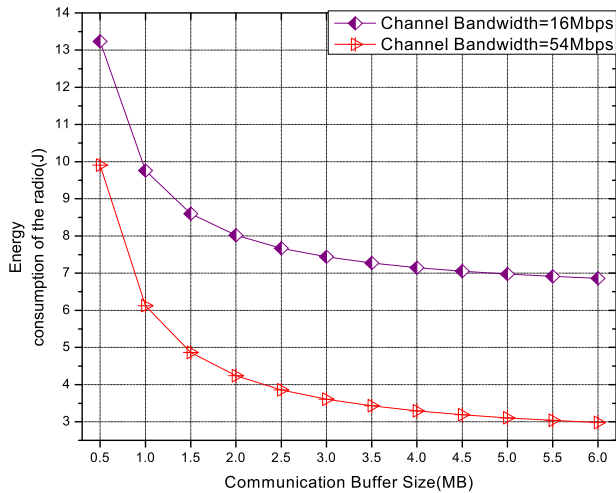


FIGURE 4. Energy consumption of radio with different buffer size.

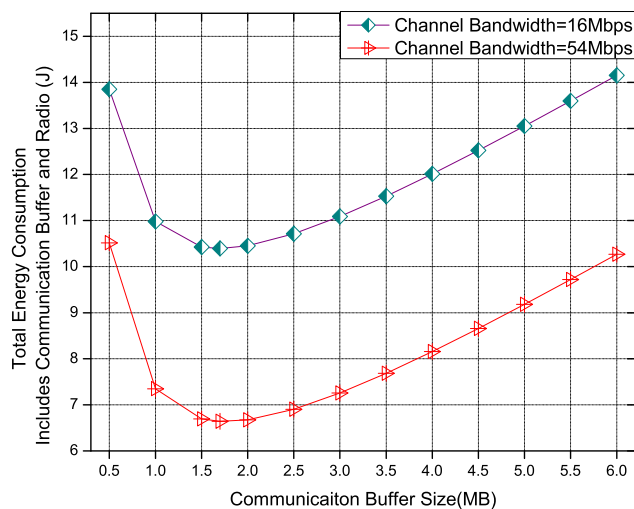


FIGURE 5. Total energy consumption of communication block with different buffer size.

Since the total energy consumption of the communication block  $\omega_{sum}$  is mainly composed of the energy consumption of the communication buffer and the energy consumption of radio, then Eq.10 and Eq.11 can be substituted into Eq.1 to obtain the Eq.12, which is the energy consumption of the communication block based on the size of the communication buffer ( $s_{sram}$ ). Here the unit of  $C_{bw}C_{vs}$  is MB.

$$\begin{aligned} \omega_{sum} = & 2 \cdot p_{ci} \cdot t_{ca} \cdot C_{vs} \cdot t_a \cdot \frac{C_{bw} - C_{vs}}{C_{bw} \cdot s_{sram}} + p_{ct} \cdot \frac{C_{vs} \cdot t_a}{C_{bw}} \\ & + 2 \cdot s_{sram} \cdot (A1 \cdot C_{vs} \cdot t_a + B1 \cdot t_a) \\ & + 2 \cdot p_{ci} \cdot t_{ca} + \frac{C_{vs} \cdot p_{ct}}{C_{bw}} \cdot \left( t_a - \frac{C_{vs} \cdot t_a}{C_{bw}} \right) \\ & + 2 \cdot A2 \cdot C_{vs} \cdot t_a + 2 \cdot B2 \cdot t_a \end{aligned} \quad (12)$$

According to the Eq. 12, the total energy consumption of communication block with different buffer size can be calculated, as shown in Figure 5.

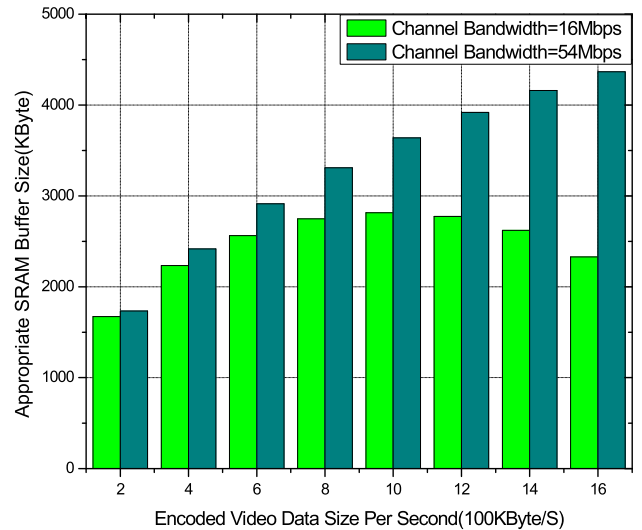


FIGURE 6. The optimum size of communication buffer under different video resolution and frame rate.

As mentioned above, the total energy consumption of the communication block is composed of the energy consumption of the communication buffer and the energy consumption of radio. The energy consumption of communication buffer is mainly related to its size and is proportional to its size, that is, the smaller the communication buffer ( $s_{sram}$ ), the smaller the energy consumption; but the energy consumption of radio is inversely proportional to the communication buffer ( $s_{sram}$ ), that is, the larger the communication buffer, the smaller the energy consumption; so we need to find a reasonable value of  $s_{sram}$  to ensure that the total energy consumption of communication model ( $\omega_{sum}$ ) is the smallest. Observing Eq.12 and Figure 5, we know that the curve of  $\omega_{sum}$  is a parabola with an upward opening, i.e. there is a minimum value. So we derive Eq.12 to make the functional derivative of  $\omega_{sum}$  zero, namely Eq.13, which can get the expression Eq.14 of optimum value of communication buffer size ( $s_{opt}$ ) by calculating conversion. Here, the value of  $s_{opt}$  corresponds to the minimum value of parabola, that is, the total energy consumption of communication module of nodes is the smallest and the network lifetime is the longest.

$$\frac{\partial \omega_{sum}}{\partial s_{sram}} = \frac{\partial (2 \cdot \omega_s + \omega_c)}{\partial s_{sram}} = 0 \quad (13)$$

$$s_{opt} = \sqrt{\frac{p_{ci} \cdot t_{ca} \cdot C_{vs} \cdot (C_{bw} - C_{vs})}{C_{bw} \cdot (2 \cdot A1 \cdot C_{vs} + B1)}} \quad (14)$$

It can be seen from Eq.14, the optimal size of communication buffer ( $s_{opt}$ ) is a function of the size of coded video data per second ( $C_{vs}$ ) and channel bandwidth ( $C_{bw}$ ). Assign different values to  $C_{vs}$  and  $C_{bw}$  respectively, we can get the corresponding  $s_{opt}$ , as shown in Figure 6. It is observed that within the range of  $C_{vs}$ ,  $s_{opt}$  increases with the increase of  $C_{bw}$  when  $C_{bw} = 54\text{Mbps}$ ; when  $C_{bw} = 16\text{Mbps}$ ,  $s_{opt}$  increases first and then decreases with the increase of  $C_{vs}$ . Figure 7 is the optimum size of communication buffer under different

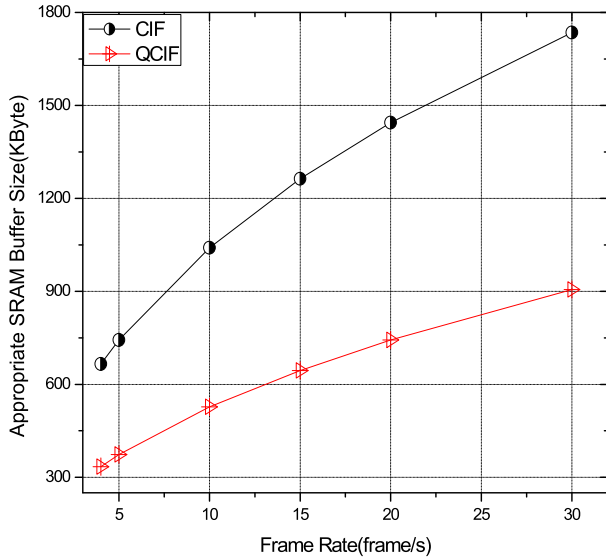


FIGURE 7. When channel bandwidth is 16Mbps, the optimum size of communication buffer under different video resolution and frame rate.

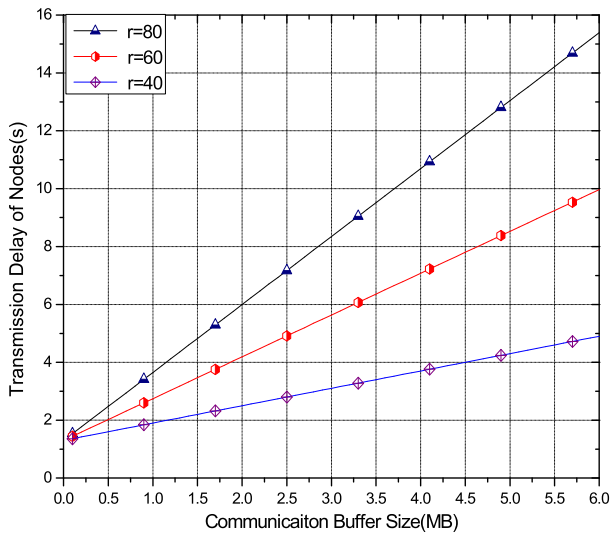


FIGURE 8. One-hop transmission delay of nodes with different buffer size.

video resolution and frame rate when the channel bandwidth is 16Mbps.

In WWSNs, the radio consumes energy even there is no data transmission during its ON state. therefore, to reduce the energy consumption, the radio is in the OFF state first, the data perceived and received by the nodes are stored in the buffer first in the process of data transmission. When the buffer is full, then the radio is turned on and transmit data to sink, the smaller the buffer size, the shorter the time is needed to fill the buffer, and the more frequently the radio is opened. The larger the buffer size, the longer the time to fill the buffer, the larger the radio startup interval, and the longer the data transmission waiting time. The relationship between the buffer size and the transmission delay can be shown in Figure 8.

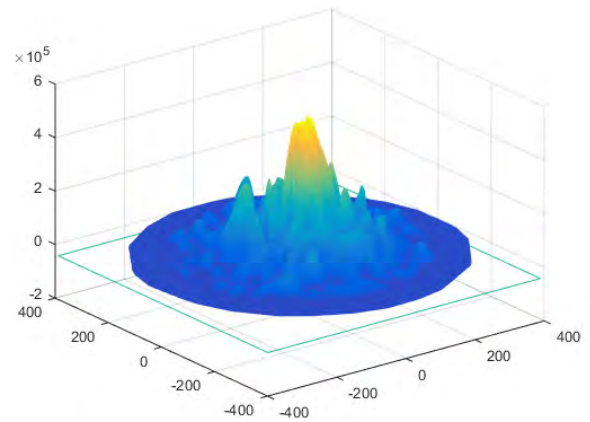


FIGURE 9. Energy consumption of the WWSN.

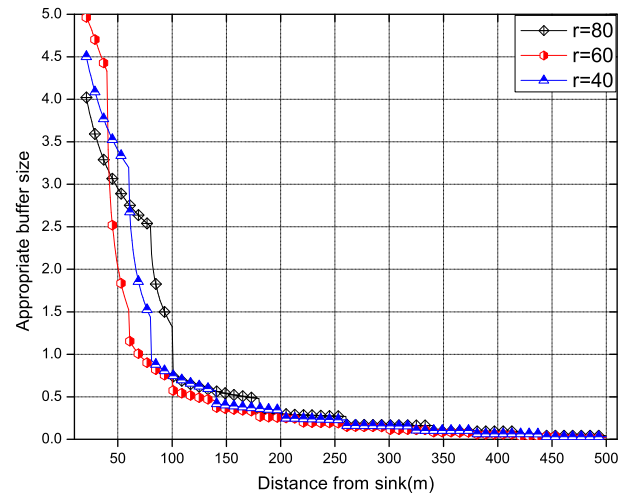


FIGURE 10. The values of communication buffers of nodes at different distances from sink.

In summary, the energy consumption of communication buffer is proportional to buffer size, while the energy consumption of radio is inversely proportional to buffer size. Therefore, an optimal value of buffer size is required to make the sum of energy consumption of the buffer and radio smallest. However, due to the close relationship between delay and buffer size, the delay is a monotonous growth with the increase of buffer size. In this case, the smaller the buffer, the better. Therefore, the two indicators are not consistent, so it is a challenge issue to optimize the delay and lifetime simultaneously.

We find that in WWSNs, the nodes near sink relay the data of far sink region, so their energy consumption is very large, while the nodes in far sink region consume less energy, so they have more energy surplus. Based on the above analysis, we can use the following methods to maintain high lifetime: using optimized buffer size in near sink region, and use a value less than the optimized buffer size in far sink region. Then, the network can maintain a high lifetime while reducing the delay.

Based on the above idea, Figure 10 gives the values of communication buffers of nodes at different distances from sink.

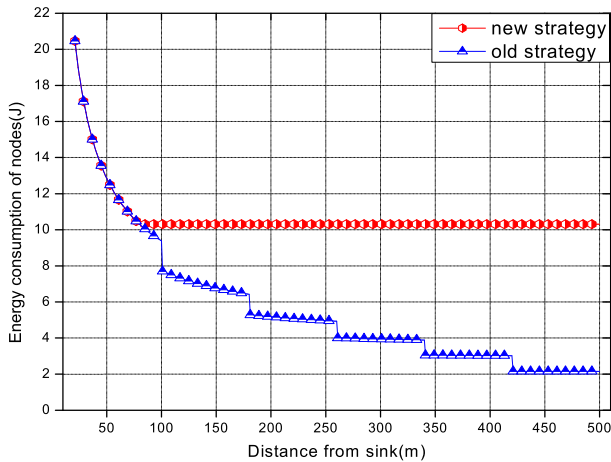


FIGURE 11. Energy consumption of nodes under the new and old strategies.

In the proposed scheme, the buffer size of nodes near sink region takes an optimal value that can make the energy consumption minimal, while nodes in far sink region take smaller values according to their energy surplus. At this time, far-sink region consumes more energy, but it reduces delay. From the point of view, the maximum energy consumption of the network is reduced, the network lifetime is not influenced, and the delay is reduced at the same time.

Figure 11 gives the energy consumption of nodes under the new and old strategies. It can be seen that in the near sink region, since buffer size is the optimal value, the energy consumption of different strategies is the same, and the lifetime of the network depends on the lifetime of the node with the highest energy consumption in the network, so the lifetime of different strategies is the same. However, because the new strategy uses small buffers in the far sink region, and there are enough energy surplus of nodes in far sink region, so increasing the energy consumption of nodes in far sink area does not affect lifetime. On the contrary, it can reduce delay. As shown in Figure 12, under the new strategy, the data transmission delays of other regional nodes are smaller than those of the old strategy except for the nodes in the near sink region. On the basis of ensuring network lifetime, the delay can be effectively reduced under the new strategy.

**B. THE DESIGN OF ADAPTION RESIZING COMMUNICATION BUFFER (ARCB) SCHEME**

In this paper, an Adaption Resizing Communication Buffer (ARCB) scheme is proposed to maximize lifetime and reduce delay for WWSNs. In ARCB scheme, the size of buffer in hotspots takes the optimal value that can make the energy consumption of the network minimal and the lifetime maximal. And the buffer size in non-hotspots takes a value that is less the optimal value to reduce delay. Although it will consume more energy for communication, due to there is a large energy surplus in the non-hotspots area, so the lifetime is not affected. Therefore, viewing from the whole network,

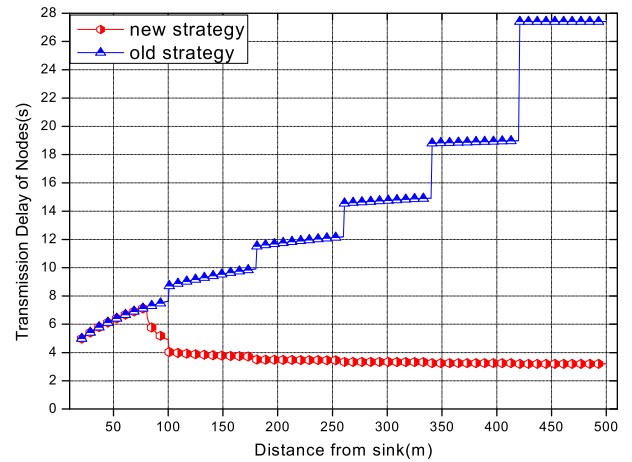


FIGURE 12. Delay of nodes under the new and old strategies.

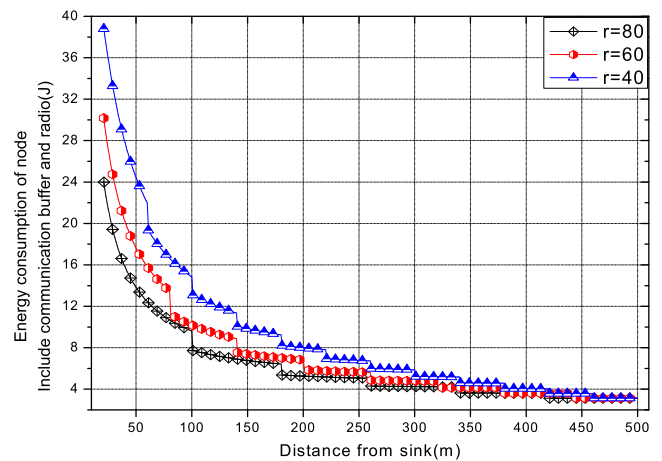


FIGURE 13. Energy consumption of nodes with different distances from the sink under the same conditions.

the aim of the ARCB scheme is to prolong the network lifetime at the same time reduce the transmission delay.

In the last section, we discussed and learned that by periodically detecting the size of video coded data per second ( $C_{vs}$ ) and the bandwidth of channel ( $C_{bw}$ ), and according to Eq.14, we can calculate the optimal size of communication buffer of nodes, and then use power gating technology to dynamically adjust it, which can minimize the energy consumption of communication block of nodes. But in the whole WWSN, as shown in Figure 13, under the same conditions, because the energy consumption of nodes in hotspots is much greater than that of nodes in the non-hotspots, when the nodes in hotspots die, the non-hotspots nodes still have a lot of energy. So we design ARCB strategy. The main idea is to adjust the size of communication buffers of nodes in different regions. For nodes in hotspots, adjust the size of communication buffers to the optimal size ( $s_{opt}$ ), and maximize the network lifetime by reducing the energy consumption of nodes. For nodes in non-hotspots, on the premise that the energy consumption of nodes is not higher than that of nodes in hotspots, adjust

the size of communication buffers according to their distance from sink. In this way, although the energy consumption is increased compared with adopting the optimal buffer size, the network lifetime is not reduced. At the same time, the transmission frequency of radio is reduced by adjusting the communication buffer size, and the transmission delay is reduced. In addition, as a contrast, we call the method that all nodes use the initial fixed size of communication buffer in previous studies as Fixed Buffer Size Adjustment strategy (FBSA), and the method of adjusting the communication buffer of all nodes to the optimal value as Optimum Buffer Size Adjustment strategy (OBSA).

In the previous part, we have calculated the optimal size of communication buffer ( $s_{opt}$ ) in hotspots. Next, we focus on how to determine the appropriate size of communication buffer of nodes with the distance of  $x$  meters from the sink, that is, the appropriate size of communication buffers  $s_x$  for nodes in non-hotspot area.

Firstly, according to the theorem in Ref. [61], assuming that the radius of the network is  $R$ , the communication radius of nodes is  $r$ , each node produces a packet in a communication cycle, and sends it to sink by the shortest path algorithm, then the data amount  $d_x$  borne by the node that is from the sink  $x$  meters can be expressed as Eq.15.

$$d_x = \left( (z + 1) + \frac{z(1+z)r}{2x} \right) \lambda \quad (15)$$

where  $z$  is the integer that can make the expression  $x+zr$  less than  $R$ , and  $\lambda$  is the probability of generating data. In this paper, the value of  $R$  is 500m, the value of  $\lambda$  is 0.1. Assume that the sink node is the circular center, then the area within the one-hop range of sink is hotspots, the data amount of nodes in hotspots can be expressed as Eq. 16.

$$d_h = \left( (z + 1) + \frac{z(1+z)}{2} \right) \lambda \quad (16)$$

**Theorem 1:** Suppose the size of communication buffer of the node from sink  $x$  meters is  $s_{xn}$ , then the energy consumption of the node can be calculated as Eq. 17.

$$\begin{aligned} \omega_x = & 2 \cdot p_{ci} \cdot t_{ca} \cdot d_x \cdot C_{vs} \cdot t_a \cdot \frac{C_{bw} - d_x \cdot C_{vs}}{C_{bw} \cdot s_{xn}} \\ & + 2 \cdot p_{ct} \cdot \frac{d_x \cdot C_{vs} \cdot t_a}{C_{bw}} + 2 \cdot s_{xn} \cdot (A1 \cdot d_x \cdot C_{vs} \cdot t_a + B1 \cdot t_a) \\ & + 2 \cdot p_{ci} \cdot t_{ca} - \frac{d_x^2 \cdot C_{vs}^2 \cdot p_{ct} \cdot t_a}{C_{bw}^2} + 2 \cdot A2 \cdot d_x \cdot C_{vs} \cdot t_a \\ & + 2 \cdot B2 \cdot t_a \quad x > r \end{aligned} \quad (17)$$

*Proof:* According to Eq. 12, the energy consumption of communication block ( $\omega_{sum}$ ) based on communication buffer size ( $s_{sram}$ ) is as follows:

$$\begin{aligned} \omega_{sum} = & 2 \cdot p_{ci} \cdot t_{ca} \cdot C_{vs} \cdot t_a \cdot \frac{C_{bw} - C_{vs}}{C_{bw} \cdot s_{sram}} + p_{ct} \cdot \frac{C_{vs} \cdot t_a}{C_{bw}} \\ & + 2 \cdot s_{sram} \cdot (A1 \cdot C_{vs} \cdot t_a + B1 \cdot t_a) + 2 \cdot p_{ci} \cdot t_{ca} \\ & + \frac{C_{vs} \cdot p_{ct}}{C_{bw}} \cdot \left( t_a - \frac{C_{vs} \cdot t_a}{C_{bw}} \right) + 2 \cdot A2 \cdot C_{vs} \cdot t_a + 2 \cdot B2 \cdot t_a \end{aligned}$$

Here, suppose the energy consumption of the node from sink  $x$  meters is  $\omega_x$ , the communication buffer size of it is  $s_{xn}$ , the data amount taken per second is  $d_x \cdot C_{vs}$ , and put the above parameters into Eq. 12, then  $\omega_x$  is obtained by replacing parameters and calculation, and Eq. 17 is proved. ■

In order to ensure the maximum network lifetime, we adjust the buffer size of nodes in hotspots to the optimal value  $s_{opt}$ , and combine with Eq.12 and the data amount  $d_h$  of nodes in hotspots to calculate the energy consumption  $\omega_h$  of nodes in hotspots, which is used as the upper limit of the energy consumption of non-hotspot nodes.

$$\begin{aligned} \omega_h = & 2 \cdot p_{ci} \cdot t_{ca} \cdot d_h \cdot C_{vs} \cdot t_a \cdot \frac{C_{bw} - d_h \cdot C_{vs}}{C_{bw} \cdot s_{opt}} \\ & + 2 \cdot p_{ct} \cdot \frac{d_h \cdot C_{vs} \cdot t_a}{C_{bw}} + 2 \cdot A2 \cdot d_h \cdot C_{vs} \cdot t_a \\ & + 2 \cdot s_{opt} \cdot (A1 \cdot d_h \cdot C_{vs} \cdot t_a + B1 \cdot t_a) + 2 \cdot p_{ci} \cdot t_{ca} \\ & - \frac{d_h^2 \cdot C_{vs}^2 \cdot p_{ct} \cdot t_a}{C_{bw}^2} + 2 \cdot B2 \cdot t_a \end{aligned} \quad (18)$$

**Theorem 2:** In ARCB scheme, suppose the upper limit of the energy consumption in non-hotspots is  $\omega_x$  ( $\omega_x = \omega_h$ ), then under the premise of maximizing lifetime and reducing delay, suppose the appropriate buffer size of the node in non-hotspots that is from the sink  $x$  meters is  $s_x$ , then  $s_x$  can be calculated as Eq. 19.

$$s_x = \frac{\omega_h - p_b - \sqrt{(\omega_h - p_b)^2 - 4 \cdot p_a \cdot p_c}}{2 \cdot p_a} \quad x > r \quad (19)$$

where

$$\begin{aligned} p_a = & 2 \cdot (A1 \cdot d_x \cdot C_{vs} \cdot t_a + B1 \cdot t_a) \\ p_c = & 2 \cdot p_{ci} \cdot t_{ca} \cdot d_x \cdot C_{vs} \cdot t_a \cdot \frac{C_{bw} - d_x \cdot C_{vs}}{C_{bw}} \\ p_b = & 2 \cdot p_{ct} \cdot \frac{d_x \cdot C_{vs} \cdot t_a}{C_{bw}} + 2 \cdot p_{ci} \cdot t_{ca} - \frac{d_x^2 \cdot C_{vs}^2 \cdot p_{ct} \cdot t_a}{C_{bw}^2} \\ & + 2 \cdot A2 \cdot d_x \cdot C_{vs} \cdot t_a + 2 \cdot B2 \cdot t_a \end{aligned}$$

*Proof:* According to Eq. 17,  $\omega_x = 2 \cdot p_{ci} \cdot t_{ca} \cdot d_x \cdot C_{vs} \cdot t_a \cdot \frac{C_{bw} - d_x \cdot C_{vs}}{C_{bw} \cdot s_{xn}} + 2 \cdot p_{ct} \cdot \frac{d_x \cdot C_{vs} \cdot t_a}{C_{bw}} + 2 \cdot s_{xn} \cdot (A1 \cdot d_x \cdot C_{vs} \cdot t_a + B1 \cdot t_a) + 2 \cdot p_{ci} \cdot t_{ca} - \frac{d_x^2 \cdot C_{vs}^2 \cdot p_{ct} \cdot t_a}{C_{bw}^2} + 2 \cdot A2 \cdot d_x \cdot C_{vs} \cdot t_a + 2 \cdot B2 \cdot t_a$ .

In ARCB scheme, suppose the energy consumption of nodes in non-hotspots does not exceed the energy consumption of nodes at the distance of one hop from sink, then it will not reduce the network lifetime but improve the utilization of residual energy in the network, at the same time make the delay smaller. Through calculation and analysis, the closer the node energy consumption is to the node energy consumption at the distance of one hop from sink, the smaller the delay. Therefore, let  $\omega_x = \omega_h$ ,  $s_x$  is obtained by calculating, transformation and formula deformation, and Eq. 19 is proved. ■

When the image parameters are (CIF, 30fps, 0.6bpp),  $C_{bw} = 54\text{Mbps}$ ,  $t_a = 30s$ , under the ARCB scheme, the size of the communication buffer of nodes with different distances

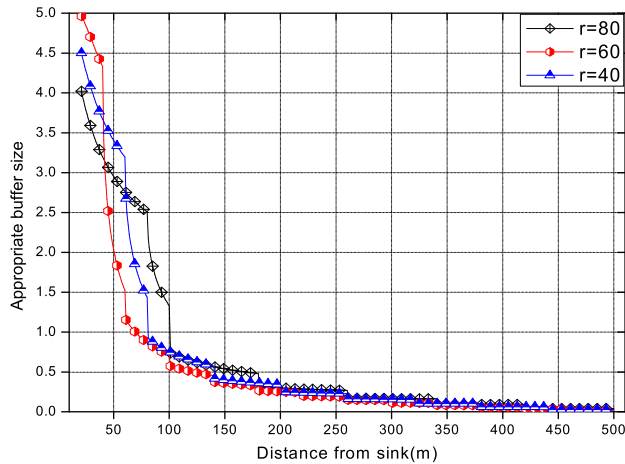


FIGURE 14. the size of communication buffer of nodes with different distances from the sink When  $r = 80$  m.

from sink is as shown in Figure 14. Keep the other parameters same, and adjust the channel bandwidth  $C_{bw}$  to 54 Mbps and 16 Mbps, respectively, then the size of the communication buffer of nodes with different distances from sink is as shown in Figure 15.

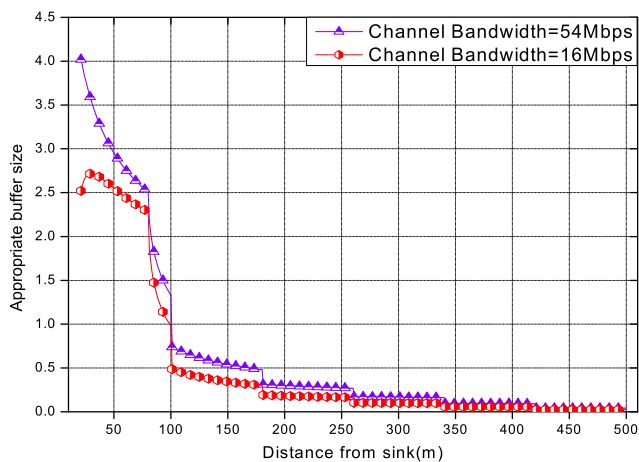


FIGURE 15. the size of communication buffer of nodes with different distances from the sink when  $C_{bw}$  is 54 Mbps and 16 Mbps,  $r = 80$  m.

*Theorem 3:* In ARCB scheme, suppose the size of communication buffer of the node from sink  $x$  meters is  $s_{xn}$ , then the one-hop transmission delay  $t_x$  of the node can be calculated as Eq. 20.

$$t_x = \frac{s_{xn}}{d_x \cdot C_{vs}} + t_{ca} + \frac{s_{xn}}{C_{bw} - d_x \cdot C_{vs}} \quad (20)$$

*Proof:* It can be seen from the above that the one-hop transmission delay of nodes includes the time of filling buffer, the start-up time of radio and the data transmission time. Combined with Eq.15, the buffer filling speed of the node from sink  $x$  meters is  $d_x \cdot C_{vs}$ , then the time required for filling data of size  $s_{xn}$  is  $\frac{s_{xn}}{d_x \cdot C_{vs}}$ . After the buffer is full, the bandwidth is  $C_{bw}$ , then the time required for transmit one-buffer-sized

data is  $t_b$ , and  $t_b$  satisfies  $t_b C_{bw} - t_b C_{vs} = s_{xn}$ , then  $t_b = s_{xn} / (C_{bw} - d_x \cdot C_{vs})$ . And the start-up time of radio is  $t_{ca}$ , and the value of  $t_{ca}$  is listed in Table 1, finally add the above three parts of time, and Eq. 20 is proved. ■

*Theorem 4:* In ARCB scheme, suppose the size of communication buffer of the node from sink  $x$  meters is  $s_{xn}$ , then the end-to-end transmission delay  $t_{xe}$  of the node can be calculated as Eq. 21.

$$t_{xe} = \sum_{i=0}^n t_{x-ir}, n = \left\lfloor \frac{x}{r} \right\rfloor \quad (21)$$

*Proof:* In WWSNs, nodes transmit data to sink via multi hops. Here, suppose the hops experienced from the node to the sink is  $n+1$ ,  $n = \left\lfloor \frac{x}{r} \right\rfloor$ , where  $x$  is the distance between the node and sink, and  $r$  the communication radius of the node. Then, the distance from each hop to the sink can be represented by  $x - ir$ , where  $i$  belongs to an integer from 0 to  $n$ , and according to the one-hop delay of the node ( $t_x = \frac{s_{xn}}{d_x \cdot C_{vs}} + t_{ca} + \frac{s_{xn}}{C_{bw} - d_x \cdot C_{vs}}$ ), the end-to-end delay of the node is obtained by accumulating the delay of multi hops, and Eq. 21 is proved.

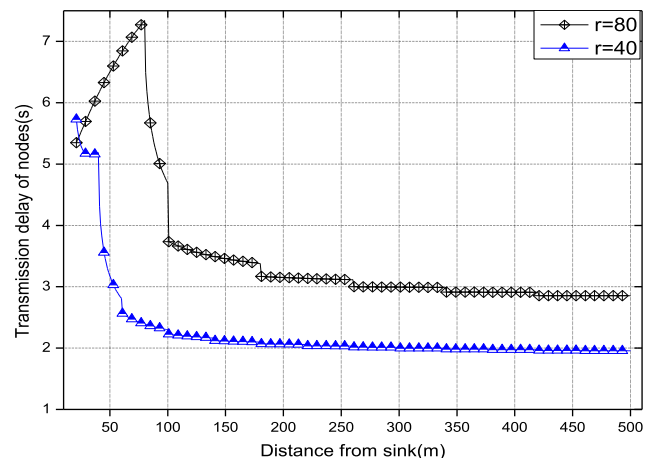


FIGURE 16. One-hop transmission delay of nodes when  $C_{bw} = 32$  Mbps.

Figure 16 and Figure 17 show that under the ARCB scheme, the one-hop transmission delay and end-to-end delay after adjusting the buffer size of nodes in hotspots to the optimal value  $s_{opt}$  and adjusting the buffer size of nodes in non-hotspots to the appropriate value  $s_x$ .

As can be seen from the above figure, the one-hop transmission delay of nodes in the hot zone is higher than that in the non-hot zone, and the end-to-end transmission delay always increases as the distance from the sink increases. Next, we compare the one-hop transmission delay and end-to-end delay of the ARCB scheme with the OBSA scheme, and in the OBSA scheme, all nodes adjusted to the optimal buffer size, as shown in Figure 18, and Figure 19.

It can be seen from the comparison that since the communication buffers in hotspots use the optimal size under both

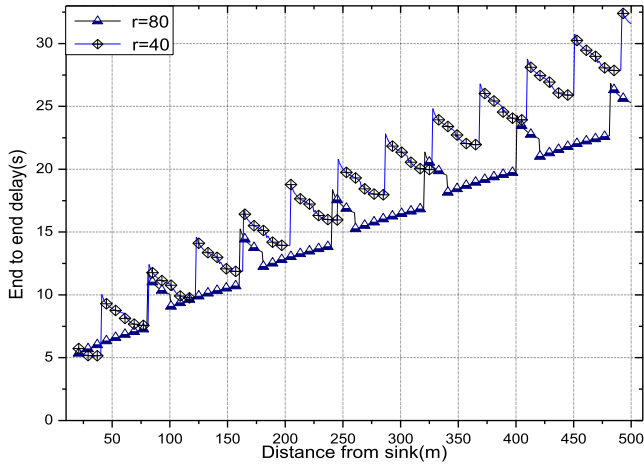


FIGURE 17. End-to-end transmission delay of nodes when  $C_{bw} = 32Mbps$ .

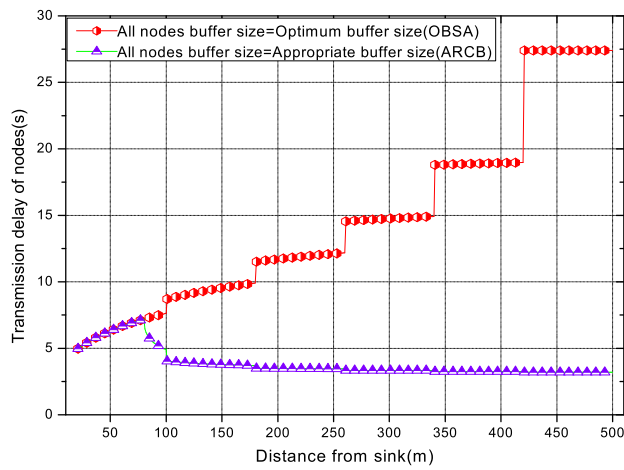


FIGURE 18. One-hop transmission delay of nodes under ARCB and OBSA scheme.

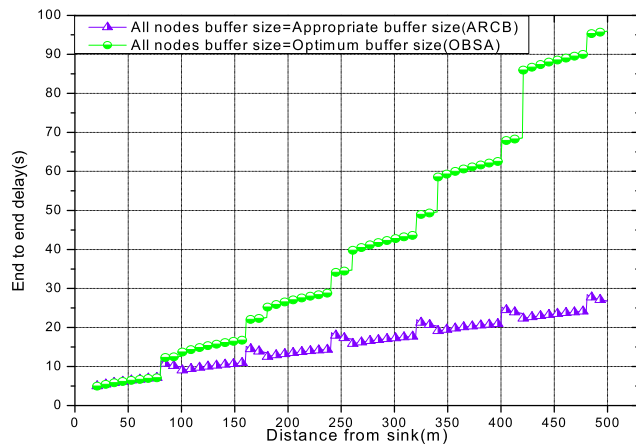


FIGURE 19. End-to-end transmission delay of nodes under ARCB and OBSA scheme.

schemes, the one-hop transmission delay and the end-to-end delay of the two schemes are the same; but as the distance from the sink increases, under the ARCB scheme, it adjust the

buffer size of nodes in non-hotspots to the appropriate size, so the one-hop transmission delay and the end-to-end delay of ARCB scheme is significantly less than OBSA scheme.

In addition, through calculation and verification, we find that under the condition of individual extreme, there are some nodes in the network edge, their communication buffer size is small, and result in the buffer filling time is less than the startup time of the radio, and the energy consumption of these node is smaller than that of hotspots, that is, Eq. 22 and Eq. 23, at this time, these nodes are converted to PIM mode for data transmission.

$$\frac{s_x}{d_x \cdot C_{vs}} < t_{ca} \tag{22}$$

$$s_x \cdot (A_1 \cdot d_x \cdot C_{vs} \cdot t_a + B_1 \cdot t_a) + A_2 \cdot d_x \cdot C_{vs} \cdot t_a + B_2 \cdot t_a + \omega_c \leq \omega_h \tag{23}$$

### V. PERFORMANCE ANALYSIS AND EXPERIMENT RESULTS

In this section, we do the experimental calculation and performance comparison analysis. Set the event duration of 30 seconds, image resolution using CIF, pixel depth of 0.6 bpp, frame rate of 30 fps, and fixed communication buffer size of 0.5 MB for persistent idle mode (PIM) and energy-saving mode (ESM). Without special explanation, other parameters are shown in Table 1.

#### A. ENERGY CONSUMPTION

##### 1) ENERGY CONSUMPTION OF NODES

Here we mainly test the energy consumption of the communication block of a single node under different modes. First, we call the mode that nodes adopt the optimal size under the ESM mode as App\_ESM mode, and the energy consumption of the communication block of nodes in App\_ESM mode is obviously lower than that of PIM and ESM mode. In the next experiment, App\_ESM calculates and adjusts the communication buffer size of nodes to the optimal value  $s_{opt}$  based on frame rate and channel bandwidth. In Figure 20, the channel bandwidth is 16Mbps, the frame rate increases from 5frame/s to 30frame/s, the energy consumption in App\_ESM mode decreases by 3%~25% compared with ESM mode, and 37%~78% compared with PIM mode. In Figure 21, the channel bandwidth is 54Mbps, the frame rate increases from 5frame/s to 30frame/s, and the total energy consumption in App\_ESM mode decreased by 3%~37% compared with ESM mode, and 57%~82% compared with PIM mode. In Figure 22, set the frame rate a fixed value of 30frame/s, the channel bandwidth is 16Mbps, and take different fixed value of buffer size, due to the optimal buffer size in App\_ESM mode depends on the channel bandwidth and the mount of video coded data per second, so under different buffer size, the total energy consumption of communication block in App\_ESM mode is the same. Compare with method before improvement, the energy consumption in App\_ESM mode decreases by 0.3%~25% compared with ESM mode, and 37%~50% compared with PIM mode. In Figure 23, except

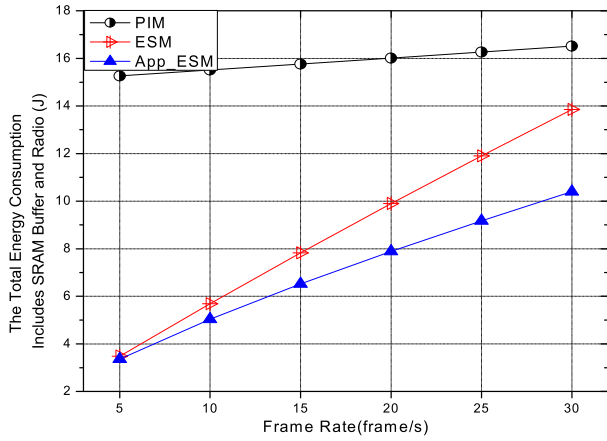


FIGURE 20.  $C_{bw} = 16\text{Mbps}$ , energy consumption of nodes when the frame rate increases from 5fram/s to 30frame/s.

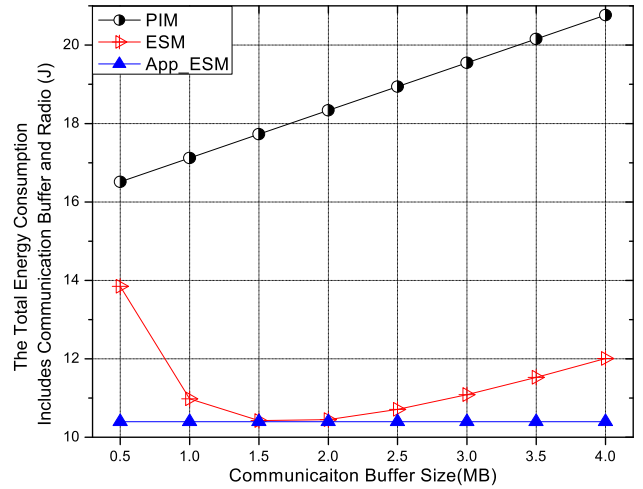


FIGURE 22.  $C_{bw} = 16\text{Mbps}$ , energy consumption of nodes when the frame rate is 30frame/s.

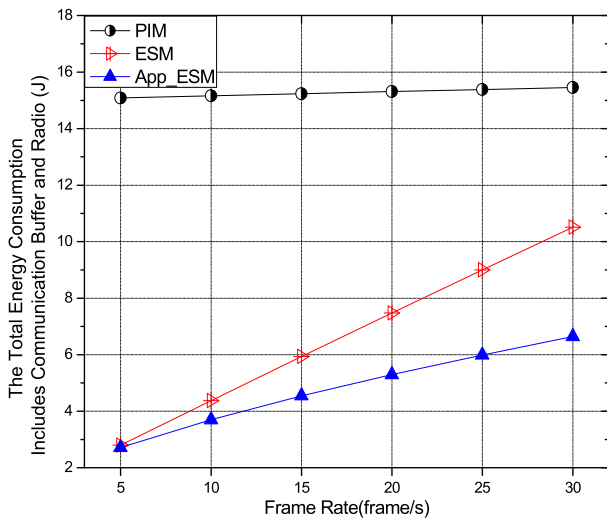


FIGURE 21.  $C_{bw} = 54\text{Mbps}$ , energy consumption of nodes when the frame rate increases from 5fram/s to 30frame/s.

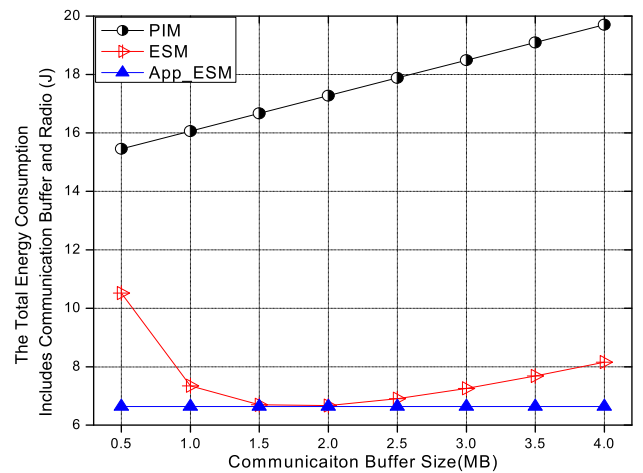


FIGURE 23.  $C_{bw} = 54\text{Mbps}$ , energy consumption of nodes when the frame rate is 30frame/s.

that the channel bandwidth is 54Mbps, the other conditions are the same as those in Figure 22, and the energy consumption in App\_ESM mode decreases by 0.4%~36% compared with ESM mode, and 57%~66% compared with PIM.

Comparing the experimental results by changing the parameters, we can see that the energy consumption in the App\_ESM mode is the lowest no matter in any case. Here, the key is to calculate the optimal value of the buffer size, because the size of communication buffer has a certain impact on its own energy consumption and the energy consumption of radio. Only choose an appropriate value can minimize the energy consumption of communication block, thereby reducing the energy consumption of nodes.

## 2) ENERGY CONSUMPTION OF THE NETWORK

Here, we analyze the energy consumption of the entire network. In the initial state, the size of the communication buffer is the same, and the value is 0.5M. Under the same conditions,

the energy consumption of nodes in different areas of the network can be obtained, as shown in Figure 24. And it can be seen from Figure 25 that the energy consumption of network is uneven, and the energy consumption of nodes in the hotspots is obviously higher than that of nodes in non-hotspots. When the first node dies, there is still a large amount of energy left by other nodes in the network, resulting in energy waste. As shown in Figure 26, the maximum residual energy can be up to 97% when dead nodes appear in the network. Therefore, the ARCB scheme proposed in this paper can improve the energy utilization by adjusting the buffer size of nodes in different areas, and make the energy consumption of nodes is basically balanced.

## B. NETWORK LIFETIME

In this section, the network lifetime under ARCB scheme is analyzed through calculation verification. Since the energy consumption of the hotspots is relatively large, and the



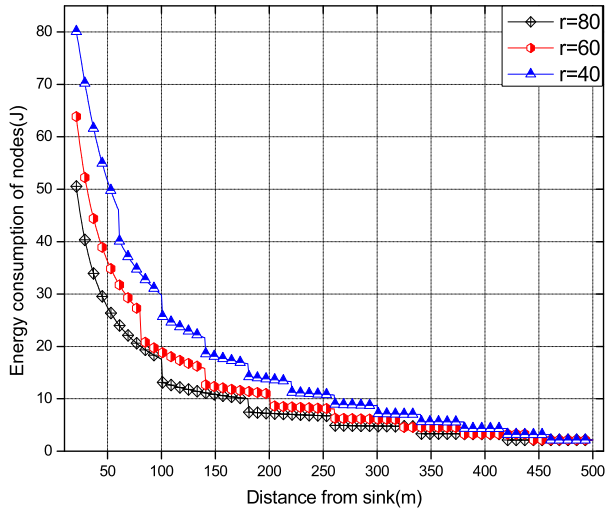


FIGURE 24. Energy consumption of nodes with different distances from the sink in WVSNs.

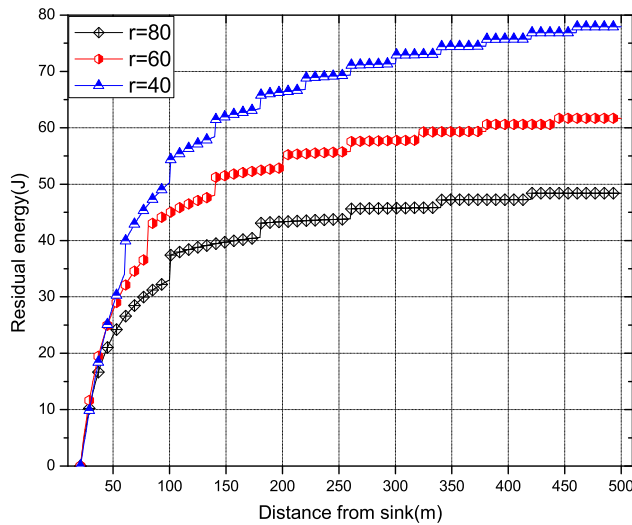


FIGURE 25. Residual energy of nodes with different distances from the sink when dead nodes appear in WVSNs.

network lifetime is defined as the death time of the first node in the network, so, we select the nodes in hotspots as the experimental objects, and compare the energy consumption of ARCB scheme, FBSA scheme and OBSA scheme, as shown is Figure 27.

As can be seen from the above figure, the energy consumption trend of ARCB scheme is the same as that of the OBSA scheme, and is much less than that of the FBSA scheme. This is because the buffer size of nodes in hotspots under ARCB scheme and OBSA scheme is adjusted to the optimal value  $s_{opt}$ , while the buffer size of nodes in hotspots under FBSA scheme is the initial value, and the energy consumption is minimal when the buffer size is adjusted to the optimal value. Next, we assume that the initial energy of each node is the same, and according to the energy consumption above, take the energy consumption of FBSA scheme as the basis

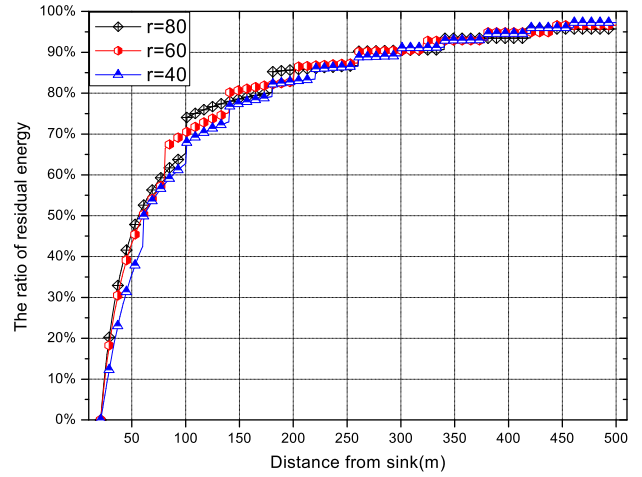


FIGURE 26. Percentage of residual energy of nodes with different distances from the sink when dead nodes appear in WVSNs.

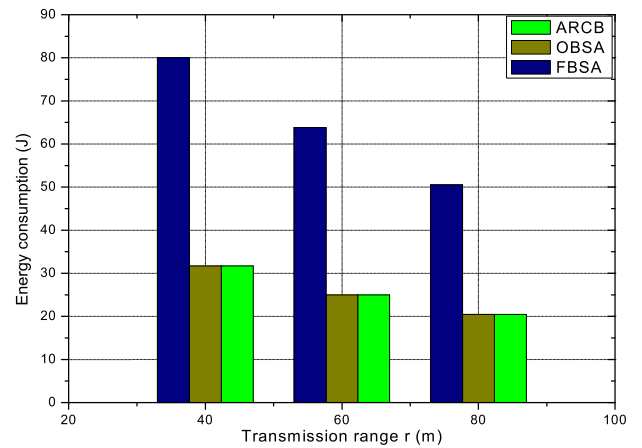


FIGURE 27. Energy consumption of nodes under different communication radius.

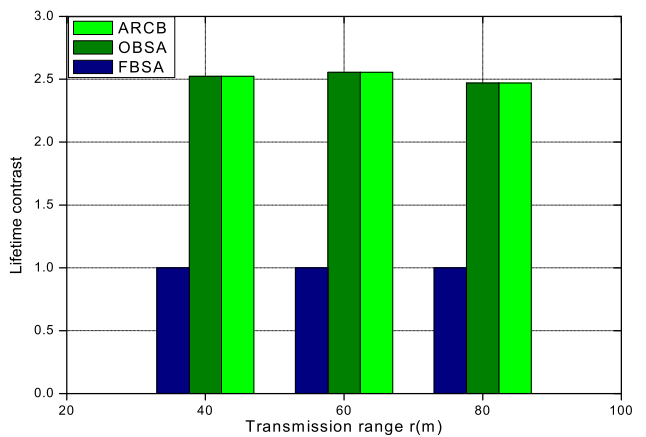


FIGURE 28. Network lifetime of ARCB, OBSA and FBSA scheme.

(its network lifetime is set to 1), and compare the lifetime under different schemes. As shown in Figure 28, under certain energy supply, the network lifetime is inversely proportional

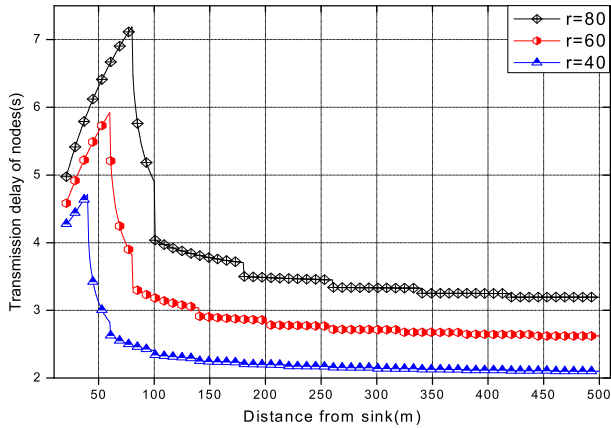


FIGURE 29. One-hop transmission delay of nodes when  $C_{bw} = 54\text{Mbps}$ .

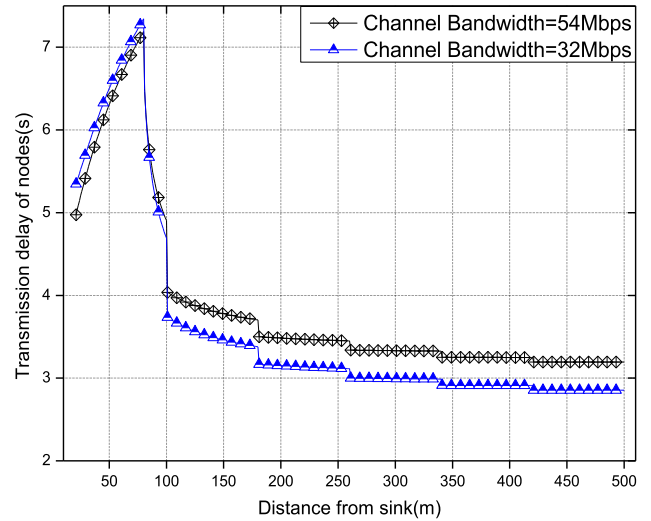


FIGURE 31. One-hop transmission delay of nodes when  $r = 80\text{m}$ .

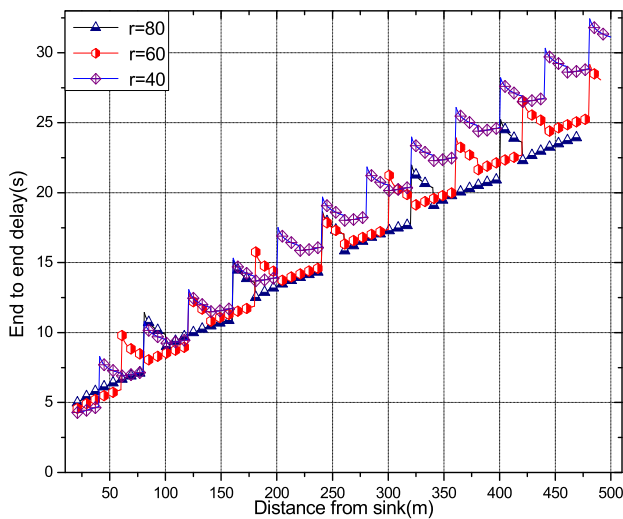


FIGURE 30. End-to-end transmission delay of nodes when  $C_{bw} = 54\text{Mbps}$ .

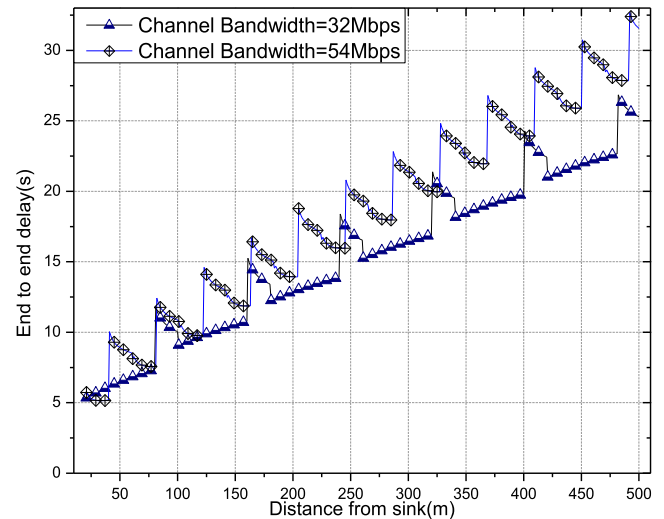


FIGURE 32. End-to-end transmission delay of nodes when  $r = 40\text{m}$ .

to energy consumption, so the network lifetime of ARCB and OBSA scheme is the same, and is much longer than the that of FBSA scheme.

### C. DELAY

This section ction mainly focuses on the analysis and comparison of the delay situations for the network nodes. Firstly, experiments and evaluations are made to verify the performances of the ARCB scheme. The duration of an event is set as 30 seconds, the image resolution of the video node to use CIF, pixel depth is 0.6 bpp, the frame rate is 30 fps and the network radius is 500 meters. The initial size of the fixed communication buffer is 0.5MB, and other parameters are shown in Table 1. The experiment targets to verify that both the one-hop transmission delay and end-to-end delay can be observed by changing the parameters and the distances from the sink in the ARCB scheme. The experimental results are shown in the Figure.29 Figure.30 Figure.31 and Figure.32 illustrate that the one-hop transmission delay in the hotspots is proportional to the distance from the sink, the

non-hotspots are inversely proportional to the distance from the sink, and the end-to-end transmission delay will increase with the increasing of the distances from the sink. This is because that in the ARCB scheme, the communication buffer of nodes in the hotspots adopts the optimum size  $s_{opt}$ , which ensures the minimum energy consumption of nodes and maximizes the network lifetime, although the transmission delay of nodes is large. The appropriate size of  $s_x$  is used for communication buffer of nodes in the non-hotspots, because the nodes in non-hotspots have residual energy, although the energy consumptions of nodes are large, it does not affect the network lifetime, and the network transmission delay is small. Therefore, the experimental results verify the effectiveness of the proposed scheme.

Then, we compare the ARCB scheme with the existing FBSA and OBSA schemes. The node delay is shown in Figure 33 and Figure. 34.with the Figure 27 and Figure 28

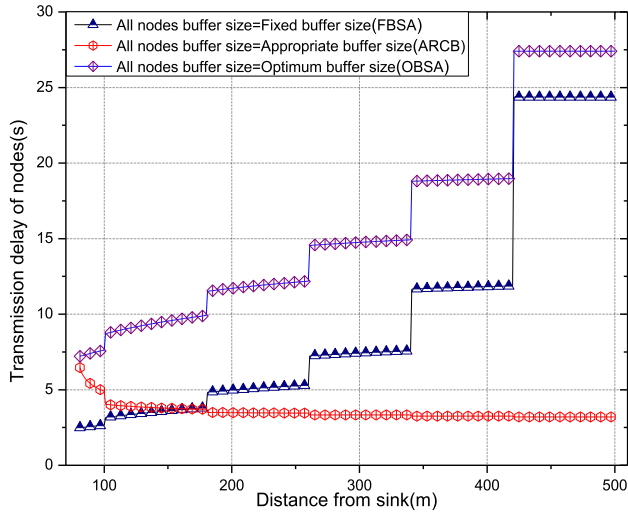


FIGURE 33. One-hop delay of ARCB, OBSA and FBSA scheme.

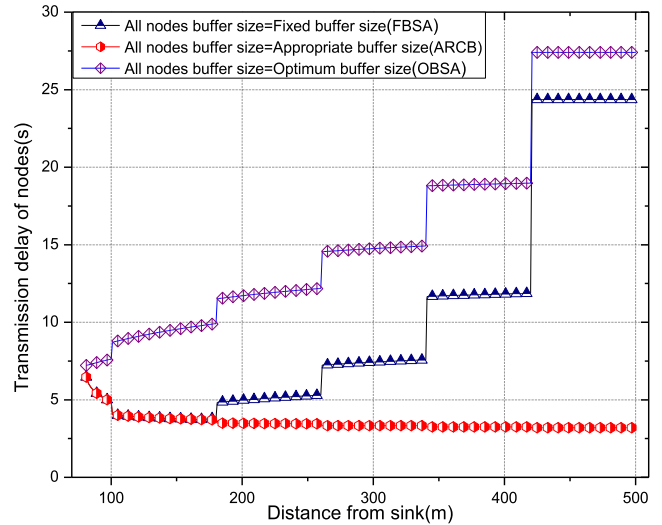


FIGURE 35. When  $C_{bw} = 54\text{Mbps}$ ,  $r = 80$ , one-hop delay of ARCB, OBSA and FBSA scheme.

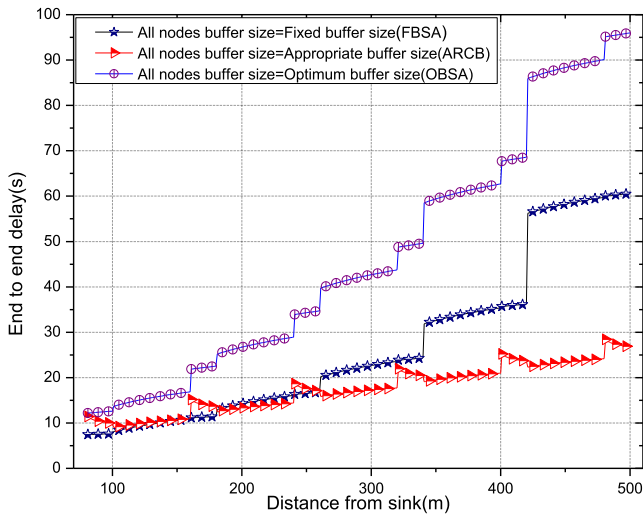


FIGURE 34. End-to-end delay of ARCB, OBSA and FBSA scheme.

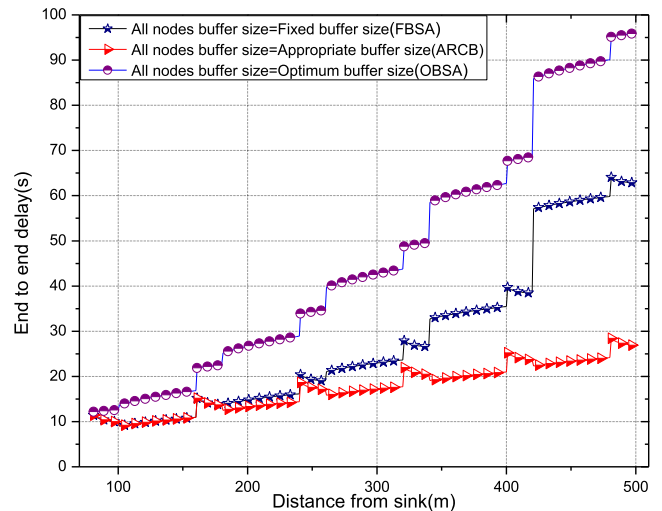


FIGURE 36. When  $C_{bw} = 54\text{Mbps}$ ,  $r = 80$ , end-to-end delay of ARCB, OBSA and FBSA scheme.

in the previous section, the FBSA scheme always keeps the communication buffer size of nodes as the initial size, the energy consumptions of nodes are large, the network lifetime is low and the delay is large; according to the network parameters, the OBSA scheme can dynamically adjust the communication buffer size of nodes to the optimal size, the energy consumptions of nodes are small, the network lifetime is high, but the delay is large; The ARCB scheme proposed in this paper can reduce the energy consumptions of nodes in the hotspots, ensure the high life of the network, and consume large energy of nodes in the non-hotspots, but it doesn't affect the life of the network, and the delay is small. Overall, ARCB scheme is superior to the existing schemes in guaranteeing the maximum network lifetime and reducing the transmission delay.

As can be seen from the figure above, the one-hop transmission delay and end-to-end delay of part nodes under FBSA scheme are less than those of ARCB scheme, that is

because the nodes outside the hotspots use the initial buffer size under the FBSA scheme. But the energy consumption of these nodes is higher than that of the nodes in the hotspots. Therefore, ARCB scheme adjusts the buffer size to reduce the energy consumption of these nodes in order to avoid the high energy consumption of these nodes, while other nodes whose energy consumption is lower than the hotspots still maintain their initial buffer size. Next, we do experiments with different parameters.

Comparing Figure 35-Figure 38, when  $C_{bw} = 54\text{Mbps}$ ,  $r=80$ , the one-hop transmission delay of ARCB scheme is 10%~88% lower than that of OBSA scheme, 1%~86% lower than that of FBSA scheme, while the end-to-end delay is 6%~72% lower than that of OBSA scheme and 0.1%~57% lower than that of FBSA scheme. When  $C_{bw} = 32\text{Mbps}$ ,  $r=40$ , the one-hop transmission delay of the ARCB scheme is reduced by 17%~92% compared to the OBSA scheme,

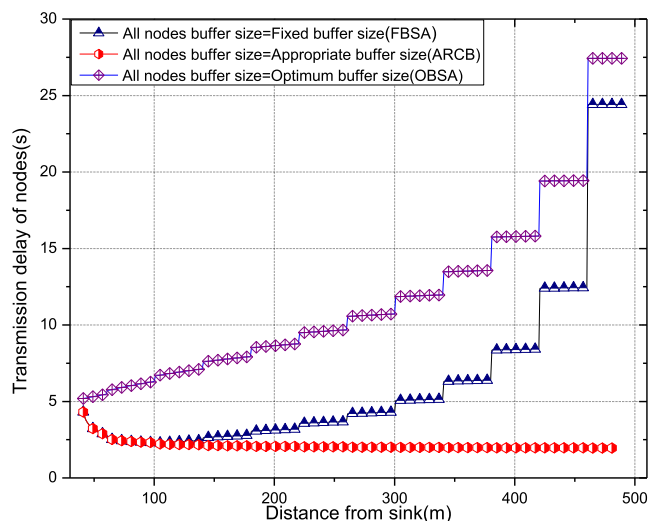


FIGURE 37. When  $C_{bw} = 32\text{Mbps}$ ,  $r = 40$ , one-hop delay of ARCB, OBSA and FBSA scheme.

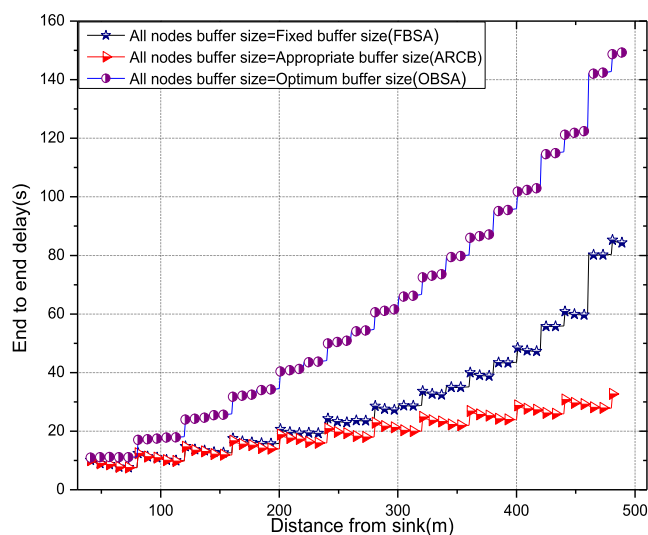


FIGURE 38. When  $C_{bw} = 32\text{Mbps}$ ,  $r = 40$ , end-to-end delay of ARCB, OBSA and FBSA scheme.

which is 2%~91% lower than the FBSA scheme, and the end-to-end delay is reduced by 8%~79% compared to the OBSA scheme, and 0.5%~63% lower than that of FBSA scheme. Obviously, the ARCB scheme has the lowest one-hop transmission delay and end-to-end delay under any network conditions, which means that the ARCB scheme proposed in this paper has a significant effect on reducing the transmission delay.

## VI. CONCLUSIONS

With the advantages of unattended, wide coverage, stable performance, high flexibility, and can achieve arbitrary combination in surveillance scenarios, Wireless Video Sensor Networks (WWSNs) has been widely used in battlefield visualization monitoring, anti-terrorism stability maintenance, environmental monitoring, security monitoring, traffic monitoring and other fields, and requirements for the network

lifetime and delay of WWSNs are also increasing important. Although there have been many studies on improving network lifetime and reducing transmission delay in the past, there are still great challenges. In view of the above situation, we propose an Adaption Resizing Communication Buffer (ARCB) scheme to maximize lifetime and reduce delay for WWSNs in this paper. Compared with FBSA scheme, in which all nodes use the initial fixed buffer sizes, ARCB scheme adjust the communication buffer size of nodes in hotspot area to the optimal size  $s_{opt}$ , thus to reduce the energy consumption of nodes and ensure the maximization of network lifetime; compared with OBSA scheme, in which all nodes use the optimal buffer sizes, on the premise of maintaining the same network lifetime, ARCB scheme adjusts the communication buffers of nodes with different distances to the appropriate size  $s_x$  by using the residual energy in the network, which improves the energy utilization and reduces the transmission delay of the nodes. Moreover, we have made a comprehensive theoretical analysis and experimental calculation of the ARCB scheme. The results fully show that the ARCB scheme is an effective and reliable scheme in terms of network lifetime and transmission delay.

## REFERENCES

- [1] R. Xiong, L. Li, Z. Li, Q. Yu, and H. Mu, "An electrochemical model based degradation state identification method of Lithium-ion battery for all-climate electric vehicles application," *Appl. Energy*, vol. 219, pp. 264–275, Jun. 2018.
- [2] D. Setiawan, A. A. Aziz, D. J. Kim, and K. W. Choi, "Experiment, modeling, and analysis of wireless-powered sensor network for energy neutral power management," *IEEE Syst. J.*, vol. 12, no. 4, pp. 3381–3392, Dec. 2018.
- [3] K. W. Choi, K. Yi, and C. M. Kyung, "Lifetime maximization of wireless video sensor network node by dynamically resizing communication buffer," *KSH Trans. Internet, Inf. Syst.*, vol. 11, no. 10, pp. 5149–5167, 2017.
- [4] X. Xiang, W. Liu, A. Liu, N. Xiong, Z. Zeng, and Z. Cai, "Adaptive duty cycle control based opportunistic routing scheme to reduce delay in Cyber physical systems," *Int. J. Distrib. Sensor Netw.*, to be published. doi: 10.1177/1550147719841870.
- [5] X. Deng et al., "Cooperative channel allocation and scheduling in multi-interface wireless mesh networks," *Peer-Peer Netw. Appl.*, vol. 12, no. 1, pp. 1–12, Jan. 2019.
- [6] Q. Liu, G. Wang, X. Liu, T. Peng, and J. Wu, "Achieving reliable and secure services in cloud computing environments," *Comput., Elect. Eng.*, vol. 59, pp. 153–164, Apr. 2017.
- [7] R. Xiong, Y. Duan, J. Cao, and Q. Yu, "Battery and ultracapacitor in-the-loop approach to validate a real-time power management method for an all-climate electric vehicle," *Appl. Energy*, vol. 217, pp. 153–165, May 2018.
- [8] Y. Liu, A. Liu, X. Liu, and X. Huang, "A statistical approach to participant selection in location-based social networks for offline event marketing," *Inf. Sci.*, vol. 480, pp. 90–108, Apr. 2019.
- [9] S. Zhang, X. Li, Z. Tan, T. Peng, and G. Wang, "A caching and spatial K-anonymity driven privacy enhancement scheme in continuous location-based services," *Future Gener. Comput. Syst.*, vol. 94, pp. 40–50, May 2019.
- [10] Q. Deng et al., "Compressed sensing for image reconstruction via back-off and rectification of greedy algorithm," *Signal Process.*, vol. 157, pp. 280–287, Apr. 2019. doi: 10.1016/j.sigpro.2018.12.007.
- [11] X. Kui, Y. Sun, S. Zhang, and Y. Li, "Characterizing the capability of vehicular fog computing in large-scale urban environment," *Mobile Netw. Appl.*, vol. 23, no. 4, pp. 1050–1067, 2018.
- [12] Y. Ren, W. Liu, T. Wang, X. Li, N. N. Xiong, and A. Liu, "A collaboration platform for effective task and data reporter selection in crowdsourcing network," *IEEE Access*, vol. 7, pp. 19238–19257, 2019.

- [13] H. Teng et al., "A novel code data dissemination scheme for Internet of Things through mobile vehicle of smart cities," *Future Gener. Comput. Syst.*, vol. 94, pp. 351–367, May 2019.
- [14] T. Li, K. Ota, T. Wang, X. Li, Z. Cai, and A. Liu, "Optimizing the coverage via the UAVs with lower costs for information-centric Internet of Things," *IEEE Access*, vol. 7, no. 1, pp. 5292–15309, 2019.
- [15] C. Xu, J. Ren, D. Zhang, Y. Zhang, Z. Qin, and K. Ren, "Ganobfuscator: Mitigating information leakage under GAN via differential privacy," *IEEE Trans. Inf. Forensics Security*, to be published. doi: [10.1109/TIFS.2019.2897874](https://doi.org/10.1109/TIFS.2019.2897874).
- [16] J. Ren, H. Guo, C. Xu, and Y. Zhang, "Serving at the edge: A scalable IoT architecture based on transparent computing," *IEEE Netw.*, vol. 31, no. 5, pp. 96–105, Aug. 2017.
- [17] H. Teng, W. Liu, T. Wang, A. Liu, X. Liu, and S. Zhang, "A cost-efficient greedy code dissemination scheme through vehicle to sensing devices (V2SD) communication in smart city," *IEEE Access*, vol. 7, pp. 16675–16694, 2019.
- [18] Y. Liu, M. Ma, X. Liu, N. Xiong, A. Liu, and Y. Zhu, "Design and analysis of probing route to defense sink-hole attacks for Internet of Things security," *IEEE Trans. Netw. Sci. Eng.*, to be published. doi: [10.1109/TNSE.2018.2881152](https://doi.org/10.1109/TNSE.2018.2881152).
- [19] X. Peng, J. Ren, L. She, D. Zhang, J. Li, and Y. Zhang, "BOAT: A block-streaming app execution scheme for lightweight IoT devices," *IEEE Internet Things J.*, vol. 5, no. 3, pp. 1816–1829, Jun. 2018.
- [20] B. Huang, W. Liu, T. Wang, X. Li, H. Song, and A. Liu, "Deployment optimization for data centers in vehicular networks," *IEEE Access*, vol. 7, no. 1, pp. 20644–20663, 2019.
- [21] Q. Liu, Y. Guo, J. Wu, and G. Wang, "Effective query grouping strategy in clouds," *J. Comput. Sci. Technol.*, vol. 32, no. 6, pp. 1231–1249, Nov. 2017.
- [22] J. Ren, Y. Zhang, N. Zhang, D. Zhang, and X. Shen, "Dynamic channel access to improve energy efficiency in cognitive radio sensor networks," *IEEE Trans. Wireless Commun.*, vol. 15, no. 5, pp. 3143–3156, May 2016.
- [23] Y. Liu, A. Liu, N. Xiong, T. Wang, and W. Gui, "Content propagation for content-centric networking from location-based social networks," *IEEE Trans. Syst., Man, Cybern., Syst.*, to be published. doi: [10.1109/TSMC.2019.2898982](https://doi.org/10.1109/TSMC.2019.2898982).
- [24] M. Huang, A. Liu, N. Xiong, T. Wang, and A. V. Vasilakos, "A low-latency communication scheme for mobile wireless sensor control systems," *IEEE Trans. Syst., Man, Cybern. Syst.*, vol. 49, no. 2, pp. 317–332, Feb. 2019.
- [25] X. Ju et al., "An energy conserving and transmission radius adaptive scheme to optimize performance of energy harvesting sensor networks," *Sensors*, vol. 18, no. 9, p. 2885, 2018. doi: [10.3390/s18092885](https://doi.org/10.3390/s18092885).
- [26] J. Tan et al., "An adaptive collection scheme based matrix completion for data gathering in energy-harvesting wireless sensor network," *IEEE Access*, vol. 7, no. 1, pp. 6703–6723, 2019.
- [27] Z. Li, Y. Liu, A. Liu, S. Wang, and H. Liu, "Minimizing convergecast time and energy consumption in green Internet of Things," *IEEE Trans. Emerg. Topics Comput.*, to be published. doi: [10.1109/TETC.2018.2844282](https://doi.org/10.1109/TETC.2018.2844282).
- [28] J. Tan et al., "A low redundancy data collection scheme to maximize lifetime using matrix completion technique," *EURASIP J. Wireless Commun. Netw.*, vol. 2019, p. 5, Jan. 2019. doi: [10.1186/s13638-018-1313-0](https://doi.org/10.1186/s13638-018-1313-0).
- [29] Z. Chen, Y. Mo, P. Ouyang, H. Shen, D. Li, and R. Zhao, "Retinal vessel optical coherence tomography images for anemia screening," *Biol. Eng. Comput.*, vol. 57, no. 4, pp. 953–966, 2019. doi: [10.1007/s11517-018-1927-8](https://doi.org/10.1007/s11517-018-1927-8).
- [30] J. Gui, Z. Li, and Z. Zeng, "Improving energy-efficiency for resource allocation by relay-aided in-band D2D communications in C-RAN-based systems," *IEEE Access*, vol. 7, pp. 8358–8375, 2018.
- [31] Z. Li, J. Gui, N. Xiong, and Z. Zeng, "Energy-efficient resource sharing scheme with out-band D2D relay-aided communications in C-RAN-based underlay cellular networks," *IEEE Access*, vol. 7, pp. 19125–19142, 2019.
- [32] A. Liu, J. Min, K. Ota, and M. Zhao, "Reliable differentiated services optimization for network coding cooperative communication system," *Int. J. Comput. Syst. Sci. Eng.*, vol. 33, no. 4, pp. 235–250, 2018.
- [33] X. Xiang, W. Liu, N. N. Xiong, H. Song, A. Liu, and T. Wang, "Duty cycle adaptive adjustment based device to device (D2D) communication scheme for WSNs," *IEEE Access*, vol. 6, pp. 76339–76373, 2018.
- [34] G. Yang, S. He, and Z. Shi, "Leveraging crowdsourcing for efficient malicious user detection in large-scale social networks," *IEEE Internet Things J.*, vol. 4, no. 2, pp. 330–339, Feb. 2017.
- [35] R. Deng, S. He, P. Cheng, and Y. Sun, "Towards balanced energy charging and transmission collision in wireless rechargeable sensor networks," *J. Commun. Netw.*, vol. 19, no. 4, pp. 341–350, 2017.
- [36] T. Wang, G. Zhang, A. Liu, MZA. Bhuiyan, Q. Jin, "A secure IoT service architecture with an efficient balance dynamics based on cloud and edge computing," *IEEE Internet Things J.*, to be published.
- [37] C. Zhang, Y. Lin, L. Zhu, A. Liu, Z. Zhang, F. Huang, "CNN-VWII: An efficient approach for large-scale video retrieval by image queries," *Pattern Recognit. Lett.*, vol. 123, pp. 82–88, May 2019.
- [38] R. Xiong, J. Cao, Q. Yu, H. He, and F. Sun, "Critical review on the battery state of charge estimation methods for electric vehicles," *IEEE Access*, vol. 6, pp. 1832–1843, 2017.
- [39] T. Wang, J. Zhou, A. Liu, M. Bhuiyan, G. Wang, and W. Jia, "Fog-based computing and storage offloading for data synchronization in IoT," *IEEE Internet Things J.*, to be published. doi: [10.1109/JIOT.2018.2875915](https://doi.org/10.1109/JIOT.2018.2875915).
- [40] X. Luo, D. Zhang, L. T. Yang, J. Liu, X. Chang, and H. Ning, "A kernel machine-based secure data sensing and fusion scheme in wireless sensor networks for the cyber-physical systems," *Future Gener. Comput. Syst.*, vol. 61, pp. 85–96, Aug. 2016.
- [41] J. Ren, Y. Zhang, K. Zhang, A. Liu, J. Chen, and X. S. Shen, "Lifetime and energy hole evolution analysis in data-gathering wireless sensor networks," *IEEE Trans. Ind. Inform.*, vol. 12, no. 2, pp. 788–800, Apr. 2016.
- [42] X. Liu, Y. Liu, N. Zhang, W. Wu, and A. Liu, "Optimizing trajectory of unmanned aerial vehicles for efficient data acquisition: A matrix completion approach," *IEEE Internet Things J.*, to be published. doi: [10.1109/JIOT.2019.2894257](https://doi.org/10.1109/JIOT.2019.2894257).
- [43] W. Liu, P. Zhuang, H. Liang, J. Peng, and Z. Huang, "Distributed economic dispatch in microgrids based on cooperative reinforcement learning," *IEEE Trans. Neural Netw. Learn. Syst.*, vol. 29, no. 6, pp. 2192–2203, Jun. 2018.
- [44] W. Qi et al., "Minimizing delay and transmission times with long lifetime in code dissemination scheme for high loss ratio and low duty cycle WSNs," *Sensors*, vol. 18, no. 10, p. 3516, 2018. doi: [10.3390/s18103516](https://doi.org/10.3390/s18103516).
- [45] Y. Liu, A. Liu, N. Zhang, X. Liu, M. Ma, and Y. Hu, "DDC: Dynamic duty cycle for improving delay and energy efficiency in wireless sensor networks," *J. Netw. Comput. Appl.*, vol. 131, pp. 16–27, Jan. 2019.
- [46] J. Li et al., "Battery-friendly based relay selection scheme to prolong lifetime for sensor nodes in Internet of Things," *IEEE Access*, vol. 7, no. 1, pp. 33180–33201, 2019.
- [47] M. Huang, W. Liu, T. Wang, H. Song, X. Li, and A. Liu, "A queuing delay utilization scheme for on-path service aggregation in services oriented computing networks," *IEEE Access*, vol. 7, pp. 23816–23833, 2019.
- [48] M. Luo, K. Wang, Z. Cai, A. Liu, Y. Li, and C. Cheang, "Using imbalanced triangle synthetic data for machine learning anomaly detection," *Comput., Mater. Continua*, vol. 58, no. 1, pp. 15–26, 2019.
- [49] C. Yang, Z. Shi, K. Han, J. J. Zhang, Y. Gu, and Z. Qin, "Optimization of particle CBMeMber filters for hardware implementation," *IEEE Trans. Veh. Technol.*, vol. 67, no. 9, pp. 9027–9031, Sep. 2018.
- [50] W. R. Heinzelman, A. Chandrakasan, and H. Balakrishnan, "Energy-efficient communication protocol for wireless microsensor networks," in *Proc. 33rd Annu. Hawaii Int. Conf. Syst. Sci.*, 2000, p. 10.
- [51] A. Liu, M. Huang, M. Zhao, and T. Wang, "A smart high-speed backbone path construction approach for energy and delay optimization in WSNs," *IEEE Access*, vol. 6, pp. 13836–13854, 2018.
- [52] R. Cristescu, B. Beferull-Lozano, and M. Vetterli, "Networked Slepian-Wolf: Theory, algorithms, and scaling laws," *IEEE Trans. Info. Theory*, vol. 51, no. 12, pp. 4057–4073, Dec. 2005.
- [53] T. Wang, A. Vosoughi, W. Heinzelman, and A. Seyedi, "Maximizing gathered samples in wireless sensor networks with Slepian-Wolf coding," *IEEE Trans. Wireless Commun.*, vol. 11, no. 2, pp. 751–761, 2012.
- [54] R. Cristescu, B. Beferull-Lozano, M. Vetterli, and R. Wattenhofer, "Network correlated data gathering with explicit communication: NP-completeness and algorithms," *IEEE/ACM Trans. Netw.*, vol. 14, no. 1, pp. 41–54, Feb. 2006.
- [55] Y. Liu et al., "FFSC: An energy efficiency communications approach for delay minimizing in Internet of Things," *IEEE Access*, vol. 4, pp. 3775–3793, 2016.
- [56] Z. Chen, A. Liu, Z. Li, Y.-J. Choi, J. Li, "Distributed duty cycle control for delay improvement in wireless sensor networks," *Peer-to-Peer Netw. Appl.*, vol. 10, no. 3, pp. 559–578, 2017.
- [57] M. Wu et al., "An effective delay reduction approach through portion of nodes with larger duty cycle for industrial WSNs," *Sensors*, vol. 18, no. 5, p. 1535, 2108. doi: [10.3390/s18051535](https://doi.org/10.3390/s18051535).
- [58] Y. Liu, A. Liu, and Z. Chen, "Analysis and improvement of send-and-wait automatic repeat-request protocols for wireless sensor networks," *Wireless Pers. Commun.*, vol. 81, no. 3, pp. 923–959, 2015.

- [59] X. Chen, M. Ma, and A. Liu, "Dynamic power management and adaptive packet size selection for IoT in e-healthcare," *Comput. Elect. Eng.*, vol. 65, pp. 357–375, Jan. 2018.
- [60] Q. Zhang and A. Liu, "An unequal redundancy level-based mechanism for reliable data collection in wireless sensor networks," *EURASIP J. Wireless Commun. Netw.*, vol. 2016, p. 258, Oct. 2016. doi: 10.1186/s13638-016-0754-6.
- [61] A. Liu, D. Zhang, P. Zhang, G. Cui, and Z. Chen, "On mitigating hotspots to maximize network lifetime in multi-hop wireless sensor network with guaranteed transport delay and reliability," *Peer-to-Peer Netw. Appl.*, vol. 7, no. 3, pp. 256–273, 2014.



**WEI ZHANG** is currently pursuing the master's degree with the School of Computer Science and Engineering, Central South University, China. His research interests include services-based networks, crowd sensing networks, and wireless sensor networks.



**WEI LIU** received the Ph.D. degree in computer application technology from Central South University, China, in 2014. He is currently an Associate Professor and a Senior Engineer with the School of Informatics, Hunan University of Chinese Medicine, China. His research interests include software engineering, data mining, and medical informatics. He has published more than 20 papers in related fields.



**TIAN WANG** received the B.Sc. and M.Sc. degrees in computer science from Central South University, in 2004 and 2007, respectively, and the Ph.D. degree from the City University of Hong Kong, in 2011. He is currently an Associate Professor with Huaqiao University, China. His research interests include wireless sensor networks, social networks, and mobile computing.



**ANFENG LIU** received the M.Sc. and Ph.D. degrees in computer science from Central South University, China, in 2002 and 2005, respectively. He is currently a Professor with the School of Computer Science and Engineering, Central South University, China. He is also a member (E200012141M) of the China Computer Federation. His current research interests include cloud computing, fog computing, and wireless sensor networks.



**ZHIWEN ZENG** is currently an Associate Professor with the School of Information Science and Engineering, Central South University, China. His current research interests include wireless sensor networks and distributed computing.



**HOUBING SONG** (M'12–SM'14) received the Ph.D. degree in electrical engineering from the University of Virginia, Charlottesville, VA, USA, in 2012. In 2017, he joined the Department of Electrical, Computer, Software, and Systems Engineering, Embry-Riddle Aeronautical University, Daytona Beach, FL, USA, where he is currently an Assistant Professor and the Director of the Security and Optimization for Networked Globe Laboratory (SONG Lab). He served on the Faculty of West Virginia University, from 2012 to 2017. In 2007, he was an Engineering Research Associate with the Texas A&M Transportation Institute. He has authored more than 100 articles. His research interests include cyber-physical systems, cybersecurity and privacy, the Internet of Things, edge computing, big data analytics, unmanned aircraft systems, connected vehicle, smart and connected health, and wireless communications and networking. He serves as an Associate Technical Editor for the *IEEE Communications Magazine*. He is an Editor of four books, including *Smart Cities: Foundations, Principles and Applications* (Hoboken, NJ, USA: Wiley, 2017), *Security and Privacy in Cyber-Physical Systems: Foundations, Principles and Applications* (Chichester, U.K.: Wiley–IEEE Press, 2017), *Cyber-Physical Systems: Foundations, Principles and Applications* (Boston, MA, USA: Academic Press, 2016), and *Industrial Internet of Things: Cybermanufacturing Systems* (Cham, Switzerland: Springer, 2016).

Dr. Song is a Senior Member of ACM. He was the very first recipient of the Golden Bear Scholar Award, the Highest Campus-Wide Recognition for Research Excellence at West Virginia University Institute of Technology, in 2016.



**SHAOBO ZHANG** received the B.Sc. and M.Sc. degrees in computer science from the Hunan University of Science and Technology, Xiangtan, China, in 2003 and 2009, respectively, and the Ph.D. degree in computer science from Central South University, Changsha, China, in 2017. He is currently a Lecturer with the School of Computer Science and Engineering, Hunan University of Science and Technology. His research interests include privacy and security issues in social networks and cloud computing.

...